THE JOURNAL OF BIOLOGICAL CHEMISTRY
Vol. 275, No. 28, Issue of July 14, pp. 21703–21714, 2000
Printed in U.S.A.

The Mammalian Peroxin Pex5pL, the Longer Isoform of the Mobile Peroxisome Targeting Signal (PTS) Type 1 Transporter, Translocates the Pex7p·PTS2 Protein Complex into Peroxisomes via Its Initial Docking Site, Pex14p*

Received for publication, January 31, 2000, and in revised form, April 13, 2000
Published, JBC Papers in Press, April 14, 2000, DOI 10.1074/jbc.M000720200

Hidenori Otera‡, Tomoyuki Harano‡, Masanori Honsho‡§, Kamran Ghaedi‡§, Satoru Mukai‡§, Atsushi Tanaka‡, Atsushi Kawai‡, Nobuhiro Shimizu‡, and Yukio Fujiki‡§¶

From the ‡Department of Biology, Kyushu University Graduate School of Science, Fukuoka 812-8581, Japan and §Core Research for Evolutional Science and Technology, Japan Science and Technology Corporation, Tokyo 170-0013, Japan

In mammals, two isoforms of the peroxisome targeting signal (PTS) type 1 receptor Pex5p, *i.e.* Pex5pS and Pex5pL with an internal 37-amino acid insertion, have previously been identified. Expression of either type of Pex5p complements the impaired PTS1 import in Chinese hamster ovary *pex5* mutants, but only Pex5pL can rescue the PTS2 import defect noted in a subgroup of *pex5* mutants such as ZP105. In this work, we found that Pex5pL directly interacts with the PTS2 receptor Pex7p, carrying its cargo PTS2 protein in the cytosol. Pex5pL, but not Pex5pS, mediated the binding of PTS2 protein to Pex14p by translocating Pex7p, demonstrating that Pex5pL plays a pivotal role in peroxisomal PTS2 import. Pex5p was localized mostly in the cytosol in wild-type CHO-K1 and Pex14p-deficient mutant cells, whereas it accumulated in the peroxisomal remnants in cell mutants defective in Pex13p or the RING family peroxins such as Pex2p and Pex12p. Furthermore, overexpression of Pex14p, but not Pex10p, Pex12p, or Pex13p, caused accumulation of Pex5p in peroxisomal membranes, with concomitant interference with PTS1 and PTS2 import. Therefore, Pex5p carrying the cargoes most likely docks with the initial site (Pex14p) in a putative import machinery, subsequently translocating to other components such as Pex13p, Pex2p, Pex10p, and Pex12p.

Peroxisomes are ubiquitous intracellular organelles that are found in organisms ranging from yeasts to human beings. The organelles are spherical, with a diameter of 0.1–1 μm, and they are bounded by a single membrane. Peroxisomes function in a wide variety of metabolic pathways, including the catabolism of very long chain fatty acids by β-oxidation and the biosynthesis of plasmalogen-type glycerolipids (1). The functional significance of human peroxisomes is highlighted by fatal human genetic diseases called peroxisome biogenesis disorders (PBDs)[1] such as Zellweger syndrome (2). Peroxisomes are formed by division of preexisting peroxisomes after post-translational import of newly synthesized proteins (3). In yeast, the endoplasmic reticulum has recently been suggested to be involved in peroxisomal membrane biogenesis (4). More than half of peroxisomal matrix proteins are mediated by well characterized *cis*-acting peroxisome targeting signals: C-terminal SKL motif PTS1 and N-terminal cleavable presequence PTS2 (2). Genetic analyses of peroxisome-deficient mutants of yeast and mammalian cells have led to the identification of a number of protein factors, peroxins, essential for peroxisome biogenesis (2, 5–7). *PEX5* and *PEX7* encoding the receptors for PTS1 and PTS2, respectively, have been identified both in yeast and mammals, including humans (for review, see Ref. 8). Deficiency of Pex5p causes PBDs of complementation group II (CG2) manifesting protein import defects (9–11).

To search for a clue to the mechanisms involved in protein import to peroxisomes, we earlier isolated two phenotypically distinct groups of *PEX5*-defective CG2 CHO cell mutants (11). One group of the *pex5* mutants, such as ZP105, showed an import defect of both PTS1 and PTS2 proteins, whereas another group of *pex5* mutants represented by ZP139 showed impaired transport of PTS1 proteins, but not PTS2 proteins. Fibroblasts with such distinct phenotypes from CG2 patients were also identified (9, 12). In yeast, *PEX5* expression complements a mutant phenotype that is defective solely in PTS1 import (13–16). In mammals, including Chinese hamster and humans, two isoforms of Pex5p, termed Pex5pS and Pex5pL, have been identified (9, 11, 12). Chinese hamster Pex5pS and Pex5pL consist of 595 and 632 amino acids, respectively (11) (see Fig. 1*E*). A G-to-A transition resulted in one amino acid substitution, G298E of Pex5pS (G335E of Pex5pL) in ZP105 and G485E of Pex5pS (G522E of Pex5pL) in ZP139 (11). Both mutations were in the tetratricopeptide repeat (TPR) domains, *i.e.* TPR1 and TPR6, respectively. In ZP105, expression of Chinese hamster (*Cl*) *PEX5S* complements import of PTS1 (but not PTS2) as in yeast, whereas *ClPEX5L* restores import of both PTS1 and PTS2, implying that Pex5pL is apparently involved in PTS2 import (11). Likewise, only Pex5pL can restore PTS2 import in fibroblasts from a CG2 patient with Zellweger syndrome (12). However, the molecular mechanisms involved in such mammalian specific import pathway(s) mediated by Pex5p are not understood.

* This work was supported in part by a CREST grant from the Japan Science and Technology Corp. (to Y. F.) and by Grants-in-aid for Scientific Research 08557011 and 09044094 from the Ministry of Education, Science, Sports, and Culture (to Y. F.). The costs of publication of this article were defrayed in part by the payment of page charges. This article must therefore be hereby marked "*advertisement*" in accordance with 18 U.S.C. Section 1734 solely to indicate this fact.

¶ To whom correspondence should be addressed: Dept. of Biology, Kyushu University Graduate School of Science, 6-10-1 Hakozaki, Higashi-ku, Fukuoka 812-8581, Japan. Tel.: 81-92-642-2635; Fax: 81-92-642-4214; E-mail: yfujiscb@mbox.nc.kyushu-u.ac.jp.

[1] The abbreviations used are: PBDs, peroxisome biogenesis disorders; PTS1 and PTS2, peroxisome targeting signal types 1 and 2, respectively; CG, complementation group; CHO, Chinese hamster ovary; TPR, tetratricopeptide repeat; GFP, green fluorescent protein; HA, hemagglutinin; RT-PCR, reverse transcription-polymerase chain reaction; GST, glutathione *S*-transferase; PAGE, polyacrylamide gel electrophoresis; PNS, post-nuclear supernatant.

Pex13p, an SH3 protein, was identified as a Pex5p-binding protein on peroxisomal membranes in yeast (17–19). Pex14p interacts with both Pex5p and Pex7p in a mammalian system (20) as well as in yeast (21, 22). Contrary to matrix proteins, import of peroxisomal membrane proteins is normal in *PEX13*-defective CHO cell mutants (23) and PBD patient fibroblasts (24, 25) and CHO *pex14* mutants (20, 26), as in most of the other mutants so far isolated (2, 27). Therefore, Pex14p and Pex13p are likely to play an important role in the import of matrix proteins, possibly as components of "import machinery."

We report herein several lines of evidence that in addition to PTS1 import, Pex5pL mediates PTS2 protein transport into peroxisomes by interaction with Pex7p and a Pex5p-docking protein, Pex14p. Intracellular location, molecular forms, and a temperature-sensitive phenotypic property of Pex5p are described. We also propose a putative peroxisomal import apparatus in relation to a mobile shuttle signal receptor, Pex5p, and its initial docking site, Pex14p.

EXPERIMENTAL PROCEDURES

Cell Culture, Transfection of PEX cDNAs, and Morphological Analysis—CHO cells were cultured as described (28). CHO-K1 cells and CHO *pex5* mutants ZP105 and ZP139 (11) (see Table I) were also cultured at 30 °C to examine a temperature-sensitive phenotype (29). In addition, we used a stable cell transformant termed 207P7,[2] which is the *PEX7*-defective CHO cell mutant ZPG207 expressing PTS2-GFP (30) that had been stably transfected with human *PEX7*. cDNA transfection was performed with expression plasmids in the pUcD2Hyg vector of CHO mutant ZP105-derived *PEX5*, *ClPEX5SG298E*, and *ClPEX5LG335E* (11). We also used influenza virus hemagglutinin (HA)-tagged *ClPEX5* variants (see below), rat *FLAG-PEX12* (31), *FLAG-ClPEX13* (23), and rat *PEX14-myc* (20), using LipofectAMINE (Life Technologies, Inc.) as described (32). Peroxisomes in CHO cells were visualized under a Carl Zeiss Axioskop FL microscope as described (11) by indirect immunofluorescence light microscopy using rabbit antibodies to PTS1 peptide (11), rat 3-ketoacyl-CoA thiolase (28), and Pex7p peptide comprising 19 amino acid residues from the C terminus.[2] PTS2-GFP in 207P7 cells was also monitored under a fluorescence microscope (30). Pex5pS and Pex5pL were detected with rabbit anti-Pex5pS antibody (see below) in cells that had been permeabilized for 5 min with either 25 μg/ml digitonin or 1% Triton X-100. Pex5p-HA (33), FLAG-Pex12p (31), FLAG-Pex13p (23), and Pex14p-Myc (20) were detected as described. Antigen-antibody complexes were detected using fluorescein isothiocyanate-labeled goat anti-rabbit IgG antibody (Cappel), except for Pex7p in 207P7, for which we used Texas Red-labeled goat anti-rabbit IgG antibody (Leinco Technologies).

Reverse Transcription-Polymerase Chain Reaction (RT-PCR)—RT-PCR was done with Superscript RT (Life Technologies, Inc.) and 5 μg of total RNA each from rat liver as well as CHO-K1 cells and *pex5* mutants ZP105 and ZP139 as described (11). Each set of primers used contained a sense and an antisense primer, respectively, as follows: 36S (5′-GGTCCTACGGTGCGGCC-3′; nucleotide sequence at positions 36–52 in *ClPEX5L* cDNA, where the initiation codon starts at position 86) (11)) and 1253R (5′-GGCTTCAGCTCCAGACA-3′; nucleotide sequence at positions 1253 to 1237) for CHO-K1; 66S (5′-GGTGGTCACCATGGCAA-3′; nucleotide sequence at positions 66–82) and 1142R (5′-TGCACTGCAGCCTCAAA-3′; nucleotide sequence at positions 1142–1126) for ZP105; and 131S (5′-AGCTGGCCACTCACTTC-3′; nucleotide sequence at positions 131–147) and 1127R (5′-AAAAGCAGCACGGCATT-3′; nucleotide sequence at positions 1127 to 1111) for ZP139. Primers used for rat liver were a sense primer (269S, 5′-AATTCCTGCAGGACCAG-3′; nucleotide sequence at positions 269–285) and an antisense primer (834R, 5′-GCCCTGCTGCTGTATAA-3′; nucleotide sequence at positions 834 to 818), designed specifically for *ClPEX5L*; another set of primers were 269S and 1268R (5′-GCTGTCCGGTTATCTGG-3′; nucleotide sequence at positions 1268 to 1252). Amplified DNA products were analyzed by agarose gel electrophoresis.

Expression of Fusion Protein—Glutathione *S*-transferase (GST) fusion protein with *ClPEX5* protein was constructed in *Escherichia coli* expression vector pGEX6P-1 (Amersham Pharmacia Biotech, Tokyo, Japan) as follows. The *Nco*I-*Bgl*II site was created in pGEX6P-1 by inserting 5′-CATGGAAGATCT-3′ and its complementary oligonucleotide into the *Sma*I site. *Nco*I-*Bgl*II fragments of pBS-*ClPEX5S* and pBS-*ClPEX5L* (11) were separately ligated into the *Nco*I-*Bgl*II site of pGEX6P-1. *Nco*I-*Bgl*II fragments, each from ZP105-derived pBS-*ClPEX5LG335E* and ZP139-type pBS-*ClPEX5LG522E* (11), were replaced into the *Nco*I-*Bgl*II site of pGEX6P-1·*ClPEX5S*. All plasmid constructs were assessed by nucleotide sequence analysis. GST fusion proteins with Chinese hamster Pex5p and rat Pex14p (20) were expressed in *E. coli* and purified as described (20). Pex5p was isolated from GST-Pex5p by cleaving with PreScission protease (Amersham Pharmacia Biotech) as described (20).

Expression of Epitope-tagged Pex5p—HA tagging to the C terminus of Pex5p was done with a PCR-based technique using a forward primer (5′-TGTCTTGGGATCCCTGTT-3′; nucleotide sequence at positions 1425–1442 in *ClPEX5L*; see above), a reverse primer (5′-GCGGCCGCTCACAATGATGCGTAATCTGGTACGTCGTATGGATAGCAGGGCAGGCCAAACATAGCT-3′) containing the HA epitope (underlined) and a stop codon, and pUcD2·*ClPEX5S* as a DNA template. HA-tagged *ClPEX5S* and *ClPEX5L* were separately cloned into pUcD2 by replacing the *Bam*HI-*Not*I fragment of each pUcD2·*ClPEX5S* and pUcD2·*ClPEX5L* with the respective *Bam*HI-*Not*I fragment of the PCR-amplified products. Plasmid pUcD2Hyg·*ClPEX5S-HA* and pUcD2Hyg·*ClPEX5L-HA* were constructed by inserting the *Bam*HI-*Not*I fragments of pUcD2·*ClPEX5S-HA* and pUcD2·*ClPEX5L-HA* into pUcD2SR-αMCSHyg·*ClPEX5S* and pUcD2SRαMCSHyg·*ClPEX5L*, respectively. All plasmid constructs were assessed by nucleotide sequence analysis and used for transfection.

In Vitro Binding Assay—The binding reaction was performed essentially as described (20). The reaction mixture (400–500 μl) contained protein components to be examined, including GST-Pex14p (3 μg), Pex5pS or Pex5pL (3 μg), ^{35}S-labeled Pex7p (10 μl), and ^{35}S-labeled-3-ketoacyl-CoA thiolase (referred to hereafter as thiolase; 10 μl) (34), in binding assay buffer (10 mM Tris-HCl, pH 7.5, 150 mM NaCl, 1% Nonidet P-40, 10% glycerol, 25 μg/ml each leupeptin and antipain, 1 mM phenylmethylsulfonyl fluoride, 1 mM EDTA, and 1 mM dithiothreitol). After incubation for 2 h at 4 °C, proteins were recovered using glutathione-Sepharose (Amersham Pharmacia Biotech), washed four times with binding assay buffer minus glycerol, and then analyzed by SDS-PAGE. Radioactive protein bands were detected using a Fujix BAS1500 Bio-Autoimaging Analyzer (Fuji Photo Film, Tokyo), and Pex5p was detected by immunoblotting. Such a GST pull-down assay was likewise done with GST fused to Pex5p or its variants derived from ZP105 and ZP139 and ^{35}S-labeled Pex7p and [^{35}S]thiolase. *In vitro* interaction assay was also performed using CHO cell lysates. CHO-K1, mutant, and 207P7 cells (1×10^8 each) were lysed on ice with binding assay buffer (2 ml) for 1 h and centrifuged at 100,000 × *g* for 40 min at 4 °C. The supernatant fraction (typically a 400-μl aliquot) was incubated with GST or GST fusion protein (~5 μg)-bound glutathione-Sepharose (30 μl) in 700 μl by rotating for 2 h at 4 °C. The Sepharose beads were washed three times with binding assay buffer minus glycerol. Bound proteins were detected by SDS-PAGE and immunoblotting. CHO-K1 cells (1×10^7) expressing Pex5pS-HA or Pex5pL-HA was likewise lysed in 2 ml, and one-fifth aliquot each was incubated with cell-free synthesized ^{35}S-labeled Pex5pS and Pex5pL (3 μl each), respectively. Pex5p-HA was immunoprecipitated with rabbit anti-HA antibody and formalin-fixed *Staphylococcus aureus* cells (Pansorbin; Calbiochem).

Co-immunoprecipitation Assay—To verify the findings *in vitro*, we conducted immunoprecipitation with anti-HA antibody using a lysate of 207P7 cells transfected with *PEX5S-HA* or *PEX5L-HA*. Co-immunoprecipitated proteins were assessed by SDS-PAGE of the immunoprecipitates, followed by immunoblotting as described below.

Gel Filtration Chromatography—To estimate the molecular mass of a Pex5p oligomer, if any, of purified recombinant Chinese hamster Pex5pS, gel filtration was performed on a Bio-Gel A-0.5m column (1 × 90 cm; Bio-Rad Japan, Tokyo) in 50 mM Hepes-KOH, pH 7.4, and 0.15 M NaCl. Molecular mass standards used were thyroglobulin (670 kDa), γ-globulin (158 kDa), ovalbumin (44 kDa), and myoglobin (17 kDa) (Bio-Rad Japan). Rat liver cytosol was isolated by centrifugation of the homogenates at 200,000 × *g* for 60 min in a Beckman Optima L-70K ultracentrifuge. The cytosol was dialyzed against 50 mM Hepes-KOH, pH 7.4, and 0.15 M NaCl then analyzed by gel filtration. Each fraction of the eluates was determined for Pex5p by SDS-PAGE and immunoblotting.

Subcellular Fractionation—CHO-K1 and peroxisome biogenesis-defective CHO cell mutants (2×10^8 each) were homogenized in 1.5 ml of homogenization buffer (0.25 M sucrose, 5 mM Hepes-KOH, pH 7.4, and 25 μg/ml each of leupeptin and antipain) by 30 strokes of an Elvehjem-Potter homogenizer. A post-nuclear supernatant (PNS) fraction, prepared by centrifugation of homogenates at 750 × *g* for 10 min, was

[2] S. Mukai and Y. Fujiki, manuscript in preparation.

centrifuged at 100,000 × *g* for 40 min to separate organelles (heavy and light mitochondrial and microsomal fractions) and the cytosol. The PNS from 1×10^7 cells was treated with 10 μg/ml proteinase K on ice for 30 min and was then separated into the organellar and cytosolic fractions. To biochemically study peroxisomal remnants, the PNS fraction from CHO mutant cells was centrifuged into a linear sucrose density gradient from 0.6 to 1.8 M in a Beckman SW 41 rotor at 35,000 rpm for 16 h at 4 °C. The gradient was collected into 23 fractions. Each fraction was analyzed by SDS-PAGE and immunoblotting.

Other Methods—For Northern blotting, RNA was isolated from CHO cells and from the livers of a rat treated for 7 days with clofibrate and an untreated rat as described (31). The RNA blot was hybridized with full-length *ClPEX5L* labeled with [α-^{32}P]dCTP (Amersham Pharmacia Biotech). *In vitro* transcription/translation was done as described (35). Antiserum to Pex5pS was raised in rabbits by conventional subcutaneous injection of bacterially expressed and purified Chinese hamster Pex5pS. Western blot analysis was done using electrophoretically transferred samples on polyvinylidene difluoride membrane (Bio-Rad) with primary antibodies, including those raised against Pex5p, rat acyl-CoA oxidase (28), rat catalase (28), human Pex7p,[3] Pex12p (31), Pex13p (23), Pex14p (20), PMP70 (70-kDa major peroxisomal integral membrane protein) from rat liver (28), and GFP (CLONTECH), and a second antibody, donkey anti-rabbit IgG antibody conjugated to horseradish peroxidase (Amersham Pharmacia Biotech). Antigen-antibody complexes were visualized with ECL Western blotting detection reagent (Amersham Pharmacia Biotech).

RESULTS

Expression of PEX5

We investigated the expression level of *PEX5* mRNA and Pex5p in rat liver and CHO cells.

Northern Blot Analysis—Peroxisomal proteins are induced in rat liver by administration of hypolipidemic agents such as clofibrate (36, 37). A rat *PEX5* mRNA band with an estimated size of ~3.3 kilobases was detected on a Northern blot of RNAs from normal and clofibrate-treated rats and was apparently not induced by clofibrate, where *PEX5S* and *PEX5L* RNAs were indistinguishable in size (Fig. 1*A*, *upper panel*, *lanes 1* and *2*). The ~3.5-kb mRNA for acyl-CoA oxidase, a PTS1 protein, was elevated ~30-fold (*middle panel*), a finding consistent with previous observations (20, 31, 37, 38). Thus, it is likely that Pex5p functions as a shuttling PTS1 receptor (see below) or in a catalytic manner, even under the conditions in which peroxisomal matrix proteins are massively induced. Alternatively, it is also plausible that the turnover rate of Pex5p is drastically altered.

RT-PCR Analysis—The expression level of *PEX5* mRNA in rat liver was also verified by RT-PCR. RT-PCR of rat RNA with a set of primers (sense primer 269S and antisense primer 834R) designed specifically for *ClPEX5L* yielded a single DNA band with an expected size from normal and clofibrate-treated rats obtained using *ClPEX5L* cDNA as a control template (Fig. 1*B*, *upper panel*). By PCR with another set of primers (269S and 1268R), giving the products from both *ClPEX5S* and *ClPEX5L*, two types of *PEX5* DNA, *i.e. PEX5S* and *PEX5L*, were obtained from rat RNA, therefore indicating that both forms of *PEX5* are expressed in rat (Fig. 1*B*, *lower panel*). Two DNA products were likewise produced with primers 494S (nucleotide sequence at positions 494–510) and 1142R (data not shown), confirming the expression of *PEX5S* and *PEX5L* mRNAs in rat.

PCR of RNA from CHO-K1 cells with a set of primers (36S and 1253R) yielded DNA of two different but expected sizes, indicating that both of the *PEX5* isoforms are expressed in CHO-K1 cells (Fig. 1*C*). The apparently larger product was more abundant than the smaller, plausibly implying that *PEX5L* mRNA is expressed at a higher level than *PEX5S* mRNA. The PCR products from CG2 *pex5* mutant ZP139-derived RNA and primers 131S and 1127R were likewise in two bands, one for *PEX5L* in a greater amount than for *PEX5S*,

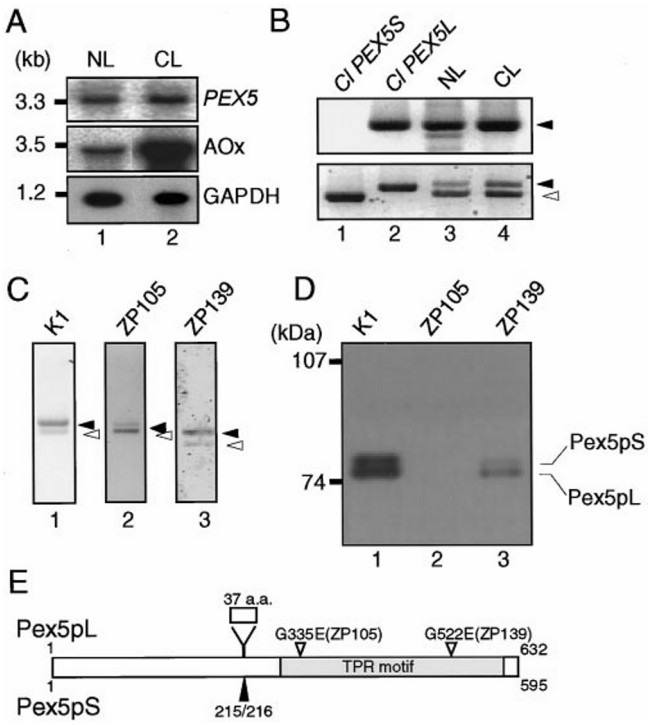

FIG. 1. **Expression levels of Pex5p in rat and CHO cells.** *A*, Northern blot analysis of liver RNA from normal and clofibrate-treated rats. RNA was separated, transferred to Zeta-Probe GT membrane (Bio-Rad), and hybridized with ^{32}P-labeled cDNA probes for *ClPEX5L* (*upper panel*) and rat acyl-CoA oxidase (*AOx*; *middle panel*). Human glyceraldehyde-3-phosphate dehydrogenase (*GAPDH*; *lower panel*) cDNA was used as a control probe to check the amount of RNA loaded. Washing was done twice with 0.3 M NaCl, 30 mM sodium citrate, and 0.5% SDS at 60 °C. *Lanes 1* and *2*, total RNAs (15 μg) from the livers of a normal (*NL*) and a clofibrate-treated (*CL*) rat, respectively. Exposure times were as follows: *upper panel*, 24 h; *middle panel*, 28 h; and *lower panel*, 24 h. *kb*, kilobases. *B*, expression level of *PEX5* mRNA. RT-PCR was done using, as templates, *ClPEX5S* (*lane 1*) and *ClPEX5L* (*lane 2*) cDNAs and total RNAs from the livers of normal (*lane 3*) and clofibrate-treated (*lane 4*) rats. PCR products were obtained with a set of primers: a forward primer (269S) and a reverse primer (834R) specific for *ClPEX5L* (*upper panel*) or primers 269S and 1268R for both *ClPEX5S* and *ClPEX5L* (*lower panel*). *C*, RT-PCR of RNA derived from wild-type and CG2 *pex5* mutant CHO cells. Cell types are designated at the top. PCR was done with total RNA from each type of cell and a set of primers: sense primer 36S and reverse primer 1253R for CHO-K1; primers 66S and 1142R for ZP105; and primers 131S and 1127R for ZP139. *Open* and *closed arrowheads* indicate the PCR products corresponding to *PEX5S* and *PEX5L*, respectively, in each cell type. *D*, expression levels of Pex5p in wild-type and *pex5* mutant CHO cells determined by immunoblotting using anti-Pex5p antibody. Cell lysates (5×10^5) were loaded in each lane; cell types are indicated at the top. To better separate Pex5pS and Pex5pL, prolonged SDS-PAGE was done. A part covering the molecular masses from 60 to 120 kDa was shown; the positions of molecular mass markers are on the left. *E*, schematic representation of Pex5pL and Pex5pS and mutation sites (G335E in ZP105 and G522E in ZP139). *215/216*, insertion site of a 37-amino acid (*a.a.*) sequence.

whereas PCR of ZP105 RNA using primers 66S and 1142R resulted in two products, more of the shorter than the longer. These results are in good agreement with findings by Northern blot analysis (11). Collectively, the two isoforms of Pex5p (Fig. 1*E*) are indeed expressed in at least three species of mammals, whereas only a single isoform is expressed in yeast.

Western Blot Analysis—The level of Pex5p in CHO-K1 cells and *pex5* (ZP105 and ZP139) was determined by immunoblotting. Pex5p was detected in CHO-K1 cells and in a lesser amount in ZP139, whereas Pex5p was under the detectable level in ZP105 cells (Fig. 1*D*), possibly due to rapidly degradation (see below). Two bands, distinct in a prolonged SDS-PAGE and showing migration with apparent masses of 78 and 80 kDa, larger than

[3] S. Mukai and Y. Fujiki, unpublished data.

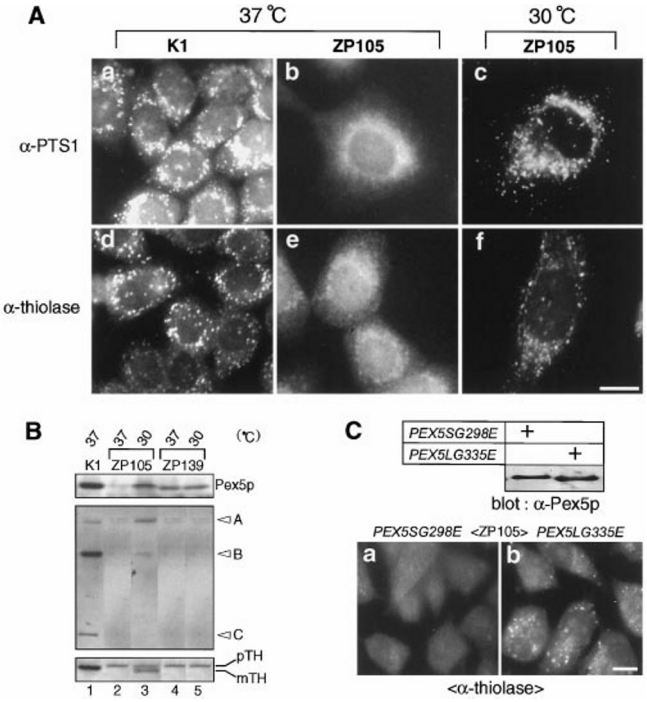

FIG. 2. **Temperature-sensitive peroxisome assembly in *pex5* mutant ZP105.** *A*, immunofluorescence staining of wild-type CHO-K1 and *pex5* mutant ZP105 cells. Cells were cultured for 3 days at 37 °C (*panels a*, *b*, *d*, and *e*) or 30 °C (*panels c* and *f*) and then stained with antibodies to PTS1 (*panels a–c*) and rat 3-ketoacyl-CoA thiolase (*panels d–f*). Magnification × 630; *bar* = 20 μm. *B*, biogenesis of peroxisomal proteins. CHO-K1 and *pex5* mutant (ZP105 and ZP139) cells (5×10^5 each) were cultured for 3 days at 37 °C (*lanes 1*, *2*, and *4*) or 30 °C (*lanes 3* and *5*). Cell lysates were subjected to SDS-PAGE and transferred to a polyvinylidene difluoride membrane. Immunoblot analysis was performed using rabbit antibodies to Pex5p (*upper panel*), rat acyl-CoA oxidase (*middle panel*), and thiolase (*lower panel*). Cell types are indicated at the top. *Arrowheads A–C* designate acyl-CoA oxidase components. *pTH* and *mTH* stand for a larger precursor and mature protein of 3-ketoacyl-CoA thiolase, respectively. *C*, back-transfection to ZP105 cells. The longer mutant isoform *PEX5LG335E* and the shorter mutant isoform *PEX5SG298E*, both derived from ZP105, were separately transfected into ZP105 cells. Cells (3×10^5 each) were verified for the expression of Pex5p by immunoblotting (*upper panel*) as well as for PTS2 import by immunostaining with anti-thiolase antibody (*lower panel*). Note that peroxisomal localization of PTS2 protein is evident in *PEX5G335E*-transfected cells (*panel b*). Magnification × 630; *bar* = 20 μm.

the calculated values from the deduced amino acid sequences (11), were noted in Pex5p from CHO-K1 cells, presumably representing two isoforms of Pex5p. The lower mobility of Pex5p in SDS-PAGE was also noted for human Pex5p (9, 10). Interestingly, Pex5pL showed a slightly greater mobility compared with Pex5pS in SDS-PAGE (see below), consistent with our earlier observation (20). The level of Pex5pL was higher than that of Pex5pS in CHO-K1 and ZP139 cells, in good agreement with the results on mRNA levels obtained by RT-PCR described above.

Temperature-sensitive Phenotype of pex5 Mutant ZP105

To examine whether CG2 *pex5* mutants show *ts* complementation of peroxisome biogenesis found in other complementation group cells such as *PEX1*-impaired CG1 patient fibroblasts (29, 39), ZP105 and ZP139 were cultured for 3 days at 30 °C. ZP105 cells were morphologically restored for peroxisome assembly with respect to the import of PTS1 and PTS2 proteins (Fig. 2*A*, *panels c* and *f*), showing apparently normal peroxisomes as in CHO-K1 cells at 37 °C (*panels a* and *d*), whereas no punctate staining was discernible at 37 °C (*panels b* and *e*). It is noteworthy that import of catalase was not restored in ZP105 after cell culture for 3 days at 30 °C (data not shown). In contrast, no PTS1- and thiolase-positive peroxisomes were found in ZP139, even at 30 °C (data not shown). Together, these data strongly suggest that the cellular phenotype of *PEX5*-defective ZP105 is *ts*.

Pex5p was hardly detectable in ZP105 when cultured for 3 days at 37 °C, whereas Pex5p was distinct in CHO-K1 cells (Fig. 2*B*, *upper panel*, *lanes 1* and *2*). After shifting to 30 °C, Pex5p was clearly discernible at 3 days of culture, as much as in ZP139 cultured at both temperatures (Fig. 2*B*, *lanes 3–5*). In normal mammalian cells, proteolytic conversion of the 75-kDa acyl-CoA oxidase A component to 53-kDa B and 22-kDa C polypeptides occurs in peroxisomes (35, 40), whereas in CHO cell mutants and PBD patient fibroblasts, the conversion of acyl-CoA oxidase fails and is instead rapidly degraded (31, 40, 41). The acyl-CoA oxidase A component was almost undetectable in ZP105 at 37 °C (Fig. 2*B*, *middle panel*, *lane 2*), presumably due to rapid degradation. The acyl-CoA oxidase A and B components were evidently increased in ZP105 cells after cell culturing for 3 days at 30 °C, indicating that the conversion of acyl-CoA oxidase proceeded in ZP105, but apparently at a slower rate compared with that in CHO-K1 cells (Fig. 2*B*, *lanes 1* and *3*). In contrast, neither the acyl-CoA oxidase A component nor its conversion was evident in ZP139, even at 30 °C (*lanes 4* and *5*), despite the normal synthesis of acyl-CoA oxidase A (11), therefore indicating a rather rapid degradation. Peroxisomal 3-ketoacyl-CoA thiolase, a PTS2 protein, is synthesized as a 44-kDa larger precursor and processed to its mature protein in peroxisomes in mammals (28, 31, 40, 41). In CHO-K1 cells, only the mature thiolase was detected at 37 °C (Fig. 2*B*, *lower panel*, *lane 1*), therefore demonstrating rapid processing of the precursor form. In ZP105, only the larger precursor was found at 37 °C as in ZP139 at both temperatures (*lanes 2*, *4*, and *5*), implying the defect in import and processing activity. When ZP105 was cultured for 3 days at 30 °C, the thiolase precursor was processed to its final size, although less efficiently compared with CHO-K1 cells (*lane 3*), reflecting the complementation of the impaired thiolase biogenesis. Taken together, these results demonstrate that cell culturing at permissive temperature can complement the abnormality in biogenesis of peroxisomal proteins in ZP105 cells, in good agreement with the morphological findings described above. Furthermore, similar but partial complementation of PTS2 import was seen at 37 °C in ZP105 cells overexpressing ZP105-derived *PEX5LG335E*, but not in those with its shorter form, *PEX5SG298E*, where nearly the same amount of both forms of mutant Pex5p was detectable with mutually distinct mobility in SDS-PAGE (Fig. 2*C*). This was interpreted to indicate that the Pex5pL G335E mutant is biologically active in PTS2 transport.

Binding of Pex5p to Peroxisomal Proteins

GST fusion proteins of both forms of wild-type Pex5p (GST-Pex5pS and GST-Pex5pL) as well as those of two types of mutant Pex5pL, one with the mutation G335E in TPR1 (GST-G335E) and the other with G522E in TPR6 (GST-G522E), from *pex5* ZP105 and ZP139 (11), respectively, were expressed in *E. coli*. Fusion protein was purified by affinity chromatography from *E. coli* lysates using a glutathione-Sepharose column. Purity of the fusion proteins was verified by SDS-PAGE (data not shown).

To investigate whether Pex5p interacts with other proteins, including several peroxins, each type of GST-Pex5p fusion protein was incubated with CHO-K1 cell lysates. Bound protein fractions were analyzed by SDS-PAGE and immunoblotting using specific antibodies. Acyl-CoA oxidase, a PTS1 protein, apparently bound to both forms of wild-type Pex5pS and Pex5pL and less efficiently to GST-G335E, but neither to GST-G522E nor to GST (Fig. 3*A*). Acyl-CoA oxidase forms oligomers

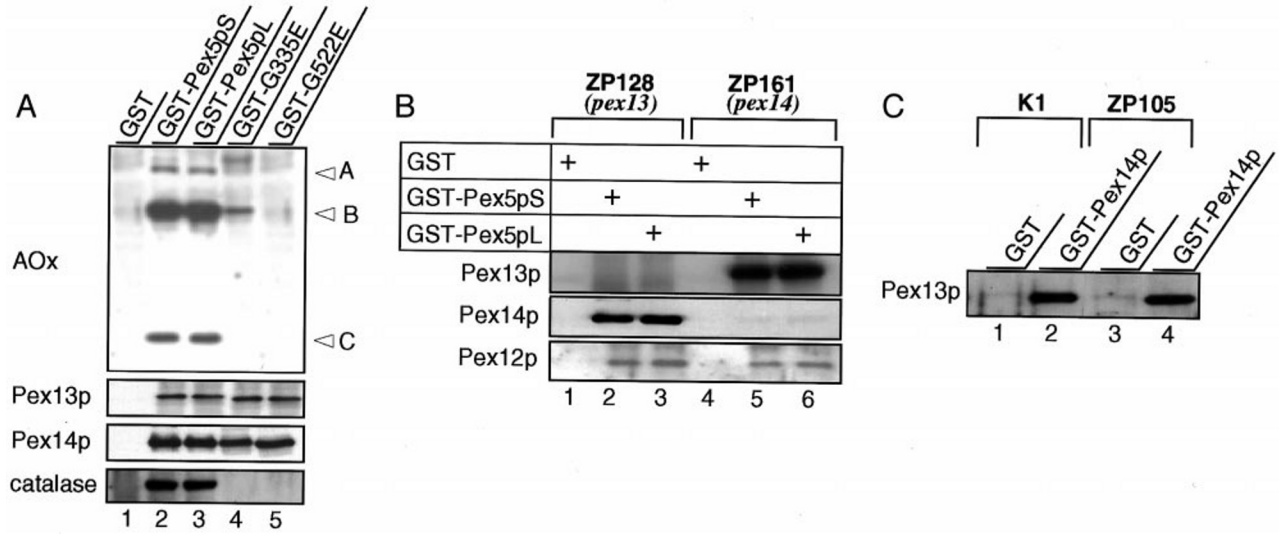

FIG. 3. **Binding of Pex5p to PTS1-related proteins and potential Pex5p-interacting peroxins.** *A*, an *in vitro* binding assay was performed using two isoforms of Pex5p from wild-type and *pex5* mutant (ZP105 and ZP139) CHO cells. GST GST-Pex5pS and GST-Pex5pL fusion proteins were separately incubated with CHO-K1 cell lysates (5×10^7 cells). GST-G335E and GST-G522E, representing GST-Pex5pL with site mutations at G335E and G522E from ZP105 and ZP139, respectively, were also used. After thorough washing, proteins bound to glutathione-Sepharose were analyzed by SDS-PAGE. Acyl-CoA oxidase (*AOx*), Pex13p, Pex14p, and catalase were probed with antibodies to the respective proteins. *B*, an *in vitro* binding assay was carried out as for *A* by incubating GST and GST-Pex5p fusion protein with *PEX13*-deficient ZP128 and *PEX14*-defective ZP161 cell lysates (5×10^7 each). Pex13p, Pex14p, and Pex12p were detected by immunoblotting. *C*, Pex5p does not mediate the interaction of Pex14p with Pex13p. GST and GST-Pex14p were separately incubated with CHO-K1 and Pex5p-deficient ZP105 cell lysates. Bound protein fractions were probed with anti-Pex13p antibody.

comprising A_2, ABC, and B_2C_2 (42). It is noteworthy that all of the three components (A, B, and C) of acyl-CoA oxidase were pulled down with GST-Pex5p, although PTS1 locates at the C termini of the A and C components. Thus, it is apparent that Pex5pS and Pex5pL recognize an oligomeric acyl-CoA oxidase, whereas Pex5pL with the mutation G335E weakly does, implicative of the *ts* phenotype of PTS1 import in ZP105. Loss of PTS1 import in ZP105 (11) appears to be due to the undetectable level of Pex5p described above. In contrast, the Pex5pL G522E mutant is severely impaired in binding to PTS1 proteins, consistent with a phenotype of ZP139 mutant cells (11). Furthermore, catalase possessing a PTS1-like C-terminal sequence, KNAL (43, 44), also bound to both forms of GST-Pex5p, but not to mutant Pex5pL (Fig. 3*A*), apparently reflecting no *ts* complementation of catalase import (see above).

Pex13p as well as Pex14p interacted with GST-Pex5pS, GST-Pex5pL, and both Pex5pL mutants, but not with GST, suggesting that both forms of wild-type Pex5p and ZP105- and ZP139-derived Pex5pL function in binding to Pex14p and Pex13p (Fig. 3*A*). PMP70, a major peroxisomal integral membrane protein, bound to none of the GST-Pex5p fusion proteins (data not shown), implying that the interaction observed above was specific. To address whether interaction of Pex5p with Pex14p requires Pex13p or *vice versa*, we used, in this binding assay, the cell lysates of *PEX13*-defective CHO mutant ZP128 (23) and *PEX14*-deficient ZP161 (20). Pex14p bound to GST-Pex5pS and GST-Pex5pL in the absence of Pex13p, and so did Pex13p in the absence of Pex14p (Fig. 3*B*). These results were interpreted to mean that Pex13p and Pex14p bind to Pex5p in an independent manner, although it is not clear whether the Pex13p-Pex5p interaction is direct or indirect. Pex12p from both cell mutants was also detected in the fractions bound to Pex5pS and Pex5pL (Fig. 3*B*).

Moreover, we investigated, using a similar assay, whether Pex14p interacts with Pex13p. Pex13p, in CHO-K1 cell lysates, bound to GST-Pex14p (Fig. 3*C*, *lane 2*). In ZP105 cell lysates in which Pex5p was at an undetectable level (see Figs. 1*D* and 2*B*), Pex13p was detected in a GST-Pex14p-bound form (Fig. 3*C*, *lane 4*). Such an interaction was not seen using GST (*lanes 1* and *3*), therefore suggesting the binding to be specific. Together, Pex13p binds directly or indirectly to Pex14p, and Pex5p does not appear to be required for the Pex13p-Pex14p interaction. However, we cannot exclude the possibility that residual Pex5p present in ZP105, if any, may be involved in such an interaction.

Oligomerization of Pex5p

To study whether Pex5pS and Pex5pL interact with themselves and/or each other, C-terminally HA-tagged Pex5pL and Pex5pS that had been expressed in Pex5p-deficient ZP105 cells were incubated with cell-free synthesized ^{35}S-labeled Pex5pS and Pex5pL and were then immunoprecipitated with anti-HA antibody. ^{35}S-Labeled Pex5pS and Pex5pL were recovered in the immunoprecipitates of Pex5pL-HA (Fig. 4*A*, *lanes 4* and *6*), suggesting that both forms of Pex5p interact with Pex5pL. Nearly the same level of ^{35}S-labeled Pex5pS and Pex5pL associated with Pex5pL, suggesting the similar affinity in the homomeric and heteromeric interaction. ^{35}S-Labeled Pex5pL and Pex5pS were likewise co-immunoprecipitated with Pex5pS-HA (*lanes 5* and *7*), confirming the findings using Pex5pL-HA. In contrast, neither Pex5pS-HA nor ^{35}S-labeled Pex5pS was discernible in the immunoprecipitate fraction from mock-transfected ZP105 (*lane 3*), indicating that the reactions noted above were specific. Similar results were likewise obtained from lysates of CHO-K1 cells expressing Pex5pL-HA or Pex5pS-HA (data not shown). Taken together, it is most likely that Pex5pS and Pex5pL form homomeric as well as heteromeric oligomers.

Chinese hamster Pex5pS purified from GST fusion protein expressed in *E. coli* was estimated in size by the gel filtration method (Fig. 4*B*). Pex5pS was eluted in a nearly single protein peak with an estimated molecular mass of ~120 kDa as assessed by absorbance at 280 nm as well as by immunoblotting, which was similar to the size of a dimeric form of the 66-kDa monomer (11). Moreover, the elution profile of Pex5p in gel filtration of rat liver cytosol, as verified by immunoblotting, was nearly the same as that of purified recombinant Chinese hamster Pex5pS, strongly suggesting that Pex5p, presumably including Pex5pL, forms a dimer (Fig. 4*B*, *lower panel*).

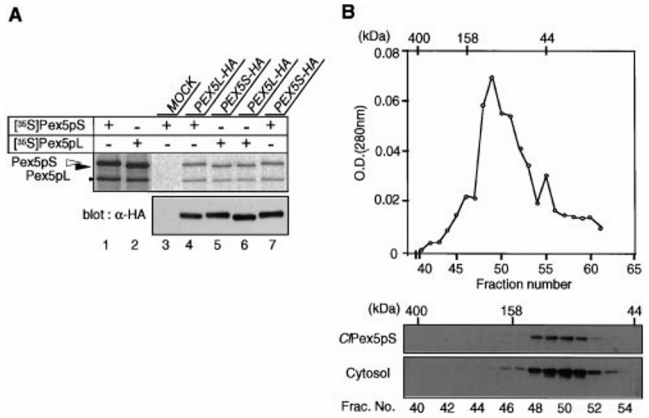

FIG. 4. **Oligomerization of Pex5p.** *A*, HA-tagged Pex5pL and Pex5pS expressed in Pex5p-deficient ZP105 cells were incubated with *in vitro* synthesized ^{35}S-labeled Pex5pS and Pex5pL and then immunoprecipitated with anti-HA antibody. Immunoprecipitates were analyzed by SDS-PAGE; ^{35}S-labeled Pex5pS and Pex5pL were detected by a Fujix BAS1500 Bio-Imaging Analyzer at an exposure of 16 h (*upper panel*). *Lanes 1* and *2*, one-fifth aliquot each of input ^{35}S-labeled Pex5pS and Pex5pL, respectively; *lane 3*, cell lysate from mock-transfected ZP105 cells incubated with ^{35}S-labeled Pex5pS; *lanes 4* and *6*, Pex5pL-HA incubated with ^{35}S-labeled Pex5pS and Pex5pL, respectively; *lanes 5* and *7*, Pex5pS-HA incubated with ^{35}S-labeled Pex5pL and Pex5pS, respectively. The *open* and *closed arrowheads* indicate Pex5pS and Pex5pL, respectively (see Fig. 1*D*); the *dot* designates a translation product presumably initiated at an internal methionine. Immunoprecipitated Pex5pS-HA and Pex5pL-HA were assessed by immunoblotting using anti-HA antibody (*lower panel*). *B*, shown are the results from gel filtration of recombinant Pex5p and rat liver Pex5p. Chinese hamster Pex5pS (230 μg) expressed in *E. coli* was analyzed by gel filtration chromatography on a Bio-Gel A-0.5m column. Each fraction of the eluates was analyzed for protein level by measuring the absorbance at 280 nm (*upper panel*). The elution positions of marker proteins are indicated at the top. Protein in each fraction (50-μl aliquot) was precipitated with 10% trichloroacetic acid and analyzed by SDS-PAGE. Rat liver cytosol (~4 mg) was similarly analyzed by chromatography and SDS-PAGE. Immunoblotting was done with anti-Pex5p antibody (*lower panels*).

Pex5pL Interacts with Pex7p

From the studies of the phenotype of *pex5* ZP105, we earlier suggested that Pex5pL is likely to be involved in PTS2 transport (11). We examined here whether Pex5p interacts with the PTS2 receptor Pex7p by the same approach described for Fig. 3. The fractions of CHO-K1 cell lysates bound to various GST-Pex5p fusion proteins were probed with rabbit anti-Pex7p antibody. Pex7p was in fractions bound to GST-Pex5pL, GST-G335E, and GST-G522E, but not to GST and GST-Pex5pS (Fig. 5*A*, *lanes 5–9*). The binding assay was performed with ^{35}S-labeled Pex7p synthesized *in vitro*. ^{35}S-Labeled Pex7p was detected after incubation only with GST-Pex5pL, strongly suggesting a direct interaction of Pex5pL with Pex7p, whereas ^{35}S-labeled Pex7p was found nearly at the background level with GST and GST-Pex5pS (*lanes 1–4*).

Pex7p was expressed at a rather low level in normal CHO-K1 and mutant cells (data not shown). To assess the Pex5p-Pex7p interaction *in vivo*, we used 207P7 cells (Table I), stable human *PEX7* transfectants of *pex7* mutant ZPG207 (30) expressing a higher level of Pex7p. Immunoprecipitation of HA-tagged Pex5pS and Pex5pL, each ectopically expressed in 207P7 cells, was done. Pex7p was detected only with Pex5pL-HA, but neither with Pex5pS-HA nor in mock-transfected cells (Fig. 5*B*), strongly suggesting that Pex5pL binds to Pex7p *in vivo*. The apparent failure of the co-immunoprecipitation of Pex7p using Pex5pS-HA can be explained. Pex7p expected, if any, in the immunoprecipitate with endogenous Pex5pL that had been bound to Pex5pS-HA is likely to be under the detectable level compared with that co-immunoprecipitated with overexpressed Pex5pL-HA. Collectively, only Pex5pL from the wild-type cells as well as from *pex5* mutants ZP105 and ZP139 functions in direct binding to Pex7p, and the mutation G335E or G522E does not affect such an interaction.

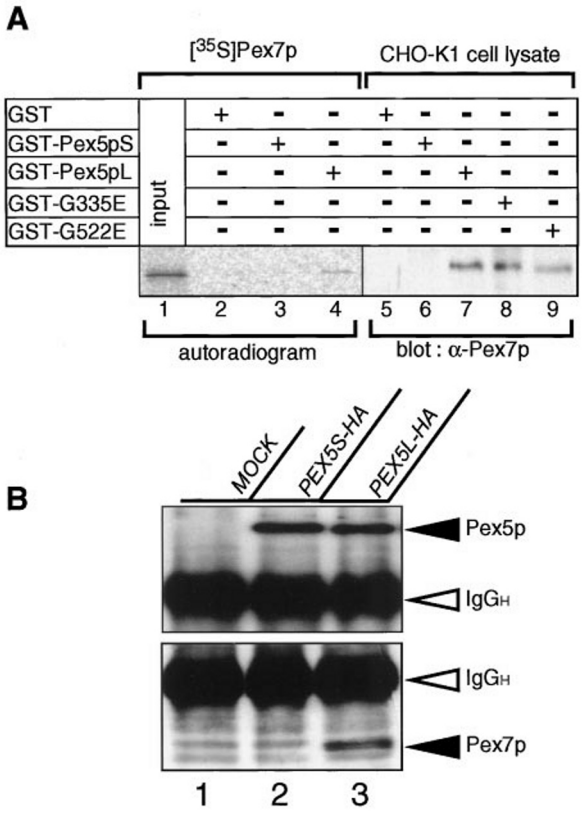

FIG. 5. **Interaction of Pex5p with Pex7p.** *A*, an *in vitro* binding assay was done using two isoforms of Pex5p from wild-type and *pex5* mutant (ZP105 and ZP139) cells and Pex7p. GST and fusion proteins GST-Pex5pS and GST-Pex5pL as well as their variants were separately incubated with ^{35}S-labeled Pex7p synthesized by cell-free transcription and translation (*lanes 2–4*) or CHO-K1 cell lysates (5×10^7 cells) (*lanes 5–9*). One-tenth aliquot of input ^{35}S-labeled Pex7p used for the assay was loaded in *lane 1*. Protein components added to the assay mixture are indicated at the top. After thorough washing, proteins bound to glutathione-Sepharose were analyzed by SDS-PAGE. ^{35}S-Labeled Pex7p was detected using a Fujix BAS1500 Bio-Imaging Analyzer at an exposure of 16 h. Pex7p endogenously expressed in CHO-K1 cells was probed with anti-Pex7p antibody. *B*, shown are the results from co-immunoprecipitation of Pex5pL with Pex7p. *ClPEX5S-HA* and *ClPEX5L-HA* were separately expressed in 207P7 cells (1×10^7 each), stable human *PEX7* transformants of *pex7* ZPG207 expressing PTS2-GFP. After a 3-day culture, Pex5p was immunoprecipitated with anti-HA antibody and analyzed by SDS-PAGE and immunoblotting. Immunoblotting was done using anti-HA antibody (*upper panel*) and anti-Pex7p antibody (*lower panel*). *Lane 1*, cell lysate from mock-transfected 207P7 cells; *lanes 2* and *3*, cell lysates from *ClPEX5S-HA*- and *ClPEX5L-HA*-transfected cells, respectively. *Closed* and *open arrowheads* indicate Pex5p (*upper closed arrowhead*) or Pex7p (*lower closed arrowhead*) and IgG heavy chain (IgG_H), respectively. A large number of IgG bands presumably interfered with the detection of PTS2-GFP, if any. Note that Pex7p is found only with Pex5pL.

TABLE I
CHO cell pex mutants used in this study and their complementing genes

pex mutant	CHO mutant	Complementing gene	Ref.
pex5	ZP105, ZP139	*PEX5*	11
pex2	Z65	*PEX2*	45
pex7	ZPG207	*PEX7*	30
pex12	ZP109	*PEX12*	31
pex13	ZP128	*PEX13*	23
pex14	ZP161	*PEX14*	20

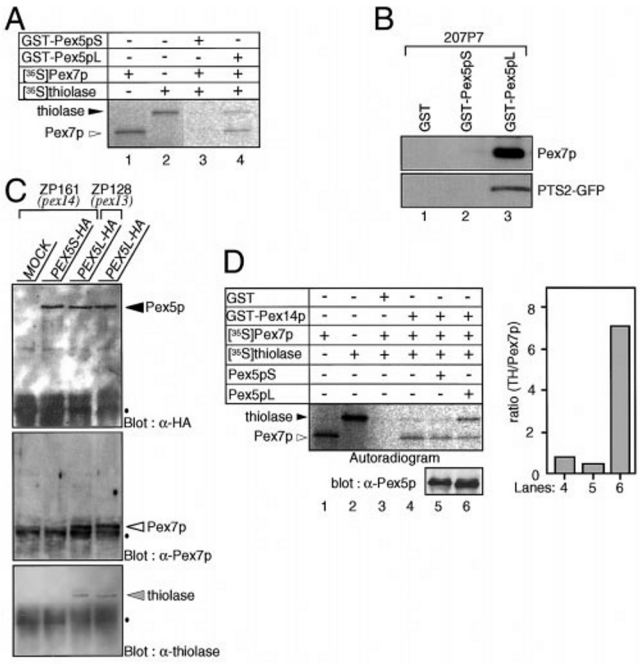

FIG. 6. **Pex5pL mediates the binding of Pex7p and PTS2 proteins to Pex14p.** *A*, an *in vitro* binding assay was performed with GST-Pex5pS, GST-Pex5pL, ^{35}S-labeled Pex7p (*open arrowhead*), and 3-ketoacyl-[^{35}S]CoA thiolase (*closed arrowhead*). One-fifth aliquot each of input ^{35}S-labeled Pex7p and [^{35}S]thiolase used for the assay was loaded in *lanes 1* and *2*, respectively. Components added to the assay mixture are indicated at the top. After thorough washing, proteins bound to glutathione-Sepharose were analyzed by SDS-PAGE. ^{35}S-Labeled Pex7p and [^{35}S]thiolase were detected as described in the legend Fig. 5 at an exposure of 14 h. *B*, an *in vitro* binding assay was done as described in the legend to Fig. 3*A* by incubating GST and GST-Pex5p fusion protein with lysates of 207P7 cells expressing a higher level of Pex7p and PTS2-GFP. Pex7p and PTS2-GFP were detected by immunoblotting using antibodies to Pex7p and GFP, respectively. *C*, shown are the results from co-immunoprecipitation of Pex5pL with Pex7p and PTS2 protein. *ClPEX5S-HA* and *ClPEX5L-HA* were separately transfected into *PEX14*-deficient ZP161, and *ClPEX5L-HA* was transfected into *PEX13*-defective ZP128. At 3 days, Pex5p was immunoprecipitated with anti-HA antibody, and the immunoprecipitates were analyzed by SDS-PAGE and immunoblotting. Immunoblotting was done using antibodies to HA (*upper panel*), Pex7p (*middle panel*), and thiolase (*lower panel*). *First lane*, immunoprecipitates using cell lysates from mock-transfected ZP161; *second* and *third lanes*, immunoprecipitates from *ClPEX5S-HA*- and *ClPEX5L-HA*-transfected ZP161, respectively; *fourth lane*, immunoprecipitates from *ClPEX5L-HA*-transfected ZP128. *Closed*, *open*, and *shaded arrowheads* indicate Pex5p, Pex7p, a precursor of thiolase, respectively. The *dot* designates an apparently nonspecific band recovered in the immunoprecipitates. Note that Pex7p as well as PTS2 thiolase were found only with Pex5pL. *D*, *left panel*, an *in vitro* binding assay was done using GST-Pex14p, purified recombinant Pex5pS and Pex5pL, ^{35}S-labeled Pex7p (*open arrowhead*), and [^{35}S]thiolase (*closed arrowhead*). One-fifth aliquot each of input ^{35}S-labeled Pex7p and [^{35}S]thiolase was loaded in *lanes 1* and *2*, respectively. Components added, including GST in place of GST-Pex14p, are indicated at the top. ^{35}S-Labeled Pex7p and [^{35}S]thiolase were detected as described for *A* at an exposure of 14 h; Pex5pS and Pex5pL were detected by immunoblotting. *Right panel*, [^{35}S]thiolase (*TH*) and Pex7p in each of *lanes 4–6* were quantitated and represented as their ratio.

Pex5pL Mediates Binding of Pex7p·PTS2 to Pex14p

To elucidate the underlying mechanisms by which Pex5pL functions in PTS2 protein transport, an *in vitro* binding assay was performed with the GST fusion proteins of Pex5pL and Pex5pS, ^{35}S-labeled Pex7p, and [^{35}S]thiolase. ^{35}S-Labeled Pex7p and [^{35}S]thiolase were detected in the fraction bound to GST-Pex5pL, whereas no ^{35}S band was associated with GST-Pex5pS (Fig. 6*A*). [^{35}S]Thiolase bound to neither GST-Pex5pL nor GST-Pex5pS (data not shown). A similar pull-down assay was performed using lysates from 207P7 cells (human *PEX7* transfectants of *pex7* ZPG207) expressing PTS2-GFP. Pex7p was detected together with PTS2-GFP using GST-Pex5pL, whereas no protein was discernible in the case of GST and GST-Pex5pS (Fig. 6*B*). Therefore, it is apparent that Pex5pL (but not Pex5pS) interacts with PTS2 protein in a Pex7p-mediated manner.

In wild-type CHO-K1 cells, unprocessed PTS2 proteins, including the peroxisomal thiolase precursor, are hardly detectable because the PTS2 signal is cleaved off in peroxisomes. Therefore, to verify *in vivo* the *in vitro* findings described above, we used CHO cell mutants in which PTS2 proteins are rather stably present at detectable levels. Pex5pS-HA and Pex5pL-HA were separately expressed in a *pex14* mutant, ZP161 (20), which is deficient in the Pex5p-docking membrane peroxin Pex14p, and then immunoprecipitated with anti-HA antibody. Pex7p and the thiolase precursor were concomitantly obtained only in the immunoprecipitates of Pex5pL, but not in those of Pex5pS or mock-transfected cells (Fig. 6*C*, *first* through *third lanes*). The same type of immunocomplex comprising Pex5pL·Pex7p·PTS2 protein was also obtained from a *pex13* mutant (ZP128) expressing Pex5pL-HA (*lane 4*). Taken together, the interaction among Pex5pL, Pex7p, and PTS2 protein apparently requires neither Pex14p nor Pex13p, both peroxisomal integral membrane proteins. Therefore, it is more likely that the Pex5pL·Pex7p·PTS2 complex is formed in the cytoplasm.

The *in vitro* pull-down assay was also done with GST-Pex14p, Pex5p, ^{35}S-labeled Pex7p, and [^{35}S]thiolase. GST-Pex14p (but not GST) bound to ^{35}S-labeled Pex7p and [^{35}S]thiolase (Fig. 6*D*, *left panel*, *lanes 3* and *4*), possibly in a Pex7p-mediated manner, as in our earlier observation using His-tagged Pex7p (20). When this binding assay was done in the presence of Pex5pS, the pull-downed ^{35}S-labeled Pex7p and [^{35}S]thiolase were slightly reduced in amount (*lane 5*) compared with those in the absence of Pex5pS. In contrast, [^{35}S]thiolase strikingly increased upon addition of Pex5pL, therefore suggesting that Pex5pL is involved in the binding of PTS2 protein to Pex14p (*lane 6*). Nearly the same level of Pex5pL as well as Pex5pS bound to Pex14p as assessed by immunoblotting using anti-Pex5p antibody (*lower panel*, *lanes 5* and *6*), where a greater migration of Pex5pL in comparison with Pex5pS was reproducibly noted as in Fig. 1*D*. Interestingly, a relatively lower level of ^{35}S-labeled Pex7p was discernible in the presence of Pex5pS or Pex5pL (*lanes 5* and *6*), although we do not know its implication at present. A specific increase in binding of [^{35}S]thiolase was determined by quantitation of the autoradiogram and was represented as the ratio to Pex7p bound to GST-Pex14p (*right panel*). A 7-fold increase was noted in the presence of Pex5pL as compared with that with only Pex7p. From several lines of evidence, including the direct interaction of Pex5pL with Pex7p (Fig. 5) and no direct binding of Pex5pL to PTS2 protein (this study and Ref. 20), it is more likely that Pex7p mediates the interaction of Pex5pL with PTS2 protein, where Pex5pL also binds to Pex14p. It is also plausible that Pex5pL enhances the binding of Pex7p to PTS2. Together, the data evidently demonstrate that Pex5pL mediates the binding of Pex7p·PTS2 protein to Pex14p, inferring that Pex5pL mediates the import of PTS2 proteins into peroxisomes.

Pex5pL Translocates Pex7p into Peroxisomes

Pex7p was morphologically detectable only in 207P7 cells, whereas it was under a detectable level in all of the other cell types investigated so far, including wild-type CHO-K1 cells.[4] To examine whether intracellular localization of Pex7p is altered by a higher level of Pex5p expression, we transfected *PEX5L-HA* as well as *PEX5S-HA* into 207P7 cells. Pex7p ap-

[4] S. Mukai and Y. Fujiki, unpublished data.

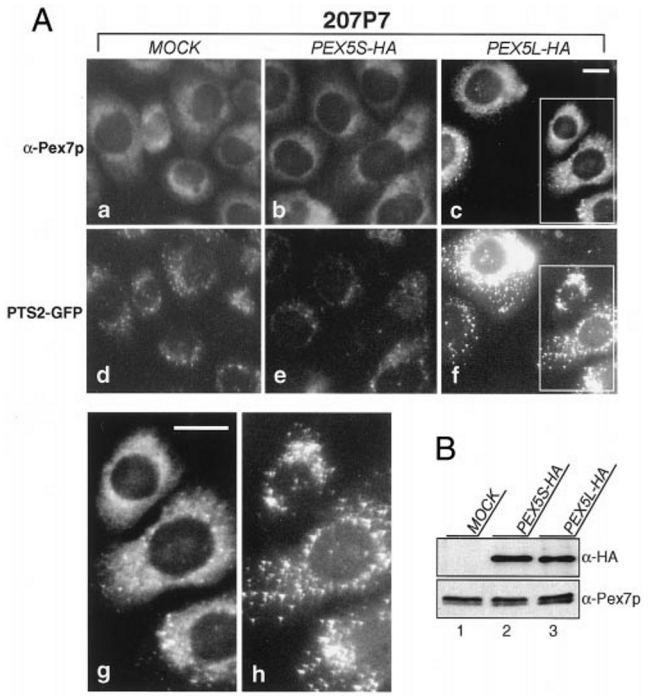

FIG. 7. **Pex5pL translocates Pex7p into peroxisomes.** HA-tagged Pex5p was expressed in 207P7 cells as described in the legend to Fig. 5*B*. *A*, transfection was performed with the vector only (*panels a* and *d*), *ClPEX5S-HA* (*panels b* and *e*), and *ClPEX5L-HA* (*panels c* and *f*). Pex7p was visualized with anti-Pex7p antibody (*panels a–c*), and PTS2-GFP was visualized by fluorescence microscopy (*panels d–f*). Cells designated in the *insets* in *panels c* and *f* are also shown at larger magnification in *panels g* and *h*, respectively. *Bars* = 20 μm. Note that Pex7p was seen partially in a punctate staining pattern, in superimposable manner with PTS2-GFP, in Pex5pL-overexpressing cells. *B*, levels of Pex5p-HA and Pex7p in each cell type were assessed by immunoblotting using antibodies to HA and Pex7p, respectively. Two protein bands immunoreactive to anti-Pex7p antibody were discernible; the one with a higher mobility is presumably the product translated from the second Met located 10 amino acids downstream of the initiator.

peared in punctate as well as cytoplasmically diffused staining patterns in Pex5pL-expressing 207P7 cells (Fig. 7*A*, *panel c*), whereas it was discernible only in the cytosol in *PEX5S*-transfected cells as in mock-transfected cells (*panels b* and *a*). Expression of Pex5pS and Pex5pL was at the same level in transfected 207P7 cells and did not affect the protein level of Pex7p (Fig. 7*B*). Although PTS2-GFP was located in peroxisomes in Pex5pS-expressing as well as untransfected cells (Fig. 7*A*, *panels d* and *e*), expression of Pex5pL strikingly enhanced the intensity of GFP-positive peroxisomes in a superimposable manner with Pex7p-positive punctates (*panels c* and *f*, *insets*; and *panels g* and *h*). The results were interpreted to mean that only Pex5pL binds to Pex7p·PTS2 and translocates them into peroxisomes. Thus, it is more likely that Pex5pL is required for peroxisome targeting of the Pex7p·PTS2 protein complex.

Intracellular Localization of Pex5p

Morphological Analysis—The intracellular localization of Pex5p was determined by immunofluorescence microscopy of CHO cells. In CHO-K1 cells, Pex5p was seen mostly in the cytosol in a diffused staining pattern with anti-Pex5p antibody (Fig. 8*A*, *panel a*). A similar localization of Pex5p was observed in a *pex14* mutant, ZP161 (20) (*panel b*). In contrast, *pex5* ZP105 cells were not stained with anti-Pex5p antibody (data not shown), consistent with an undetectable level of Pex5p expression (Fig. 1*D*). Strikingly, Pex5p was found mostly in particulates in *PEX2*-defective Z65 cells (38, 45) that had been transfected with *FLAG-PEX12* (31) (Fig. 8*A*, *panel c*). The Pex5p-positive particulate structures were superimposable with FLAG-positive particles, strongly suggesting that Pex5p is located in peroxisomal remnants or "ghosts" (40) (*panel d*). Pex5p and FLAG-Pex12p were stainable in *pex2* Z65 cells treated with 25 μg/ml digitonin, under which conditions only plasma membranes are permeabilized. Treatment of the cells with 1% Triton X-100 gave essentially the same staining pattern (data not shown). This result was interpreted to mean that Pex5p is localized on or in the membrane of the peroxisomal remnants where antibody is accessible (*panel c* and *d*). Similar punctate staining of Pex5p was discerned in *PEX12*-defective ZP109 (31) and *PEX13*-impaired ZP128 when treated with not only Triton X-100 (*panels e* and *g*), but also digitonin (*panels f* and *h*). However, Pex5p was not seen in a punctate staining pattern in ZP139 expressing both Pex5pS-G485E and Pex5pL-G522E and *PEX7*-defective ZPG207 (data not shown).

Subcellular Fractionation—The intracellular localization of Pex5p was determined also by subcellular fractionation of CHO cells. Pex5p was found by immunoblotting mostly in the cytosolic fraction and a little in organelle pellets when the PNS fraction of CHO-K1 cells was fractionated (Fig. 8*B*, *lanes 1* and *2*). In contrast, Pex5p was hardly detectable in fractions from ZP105, suggesting a degradation of Pex5p in cell culture at 37 °C (*lanes 3* and *4*), consistent with the results using total cell lysate (Figs. 1*D* and 2*B*). PMP70 was recovered exclusively in the membrane fractions of CHO-K1 and CHO cell mutants such as *pex5* ZP105 and ZP139 and *pex2* Z65, whereas catalase was largely in organelle pellets of CHO-K1, obviously in peroxisomes, and in the cytosolic fraction of the cell mutants, all consistent with our earlier morphological and biochemical findings (11, 28). Accordingly, these results confirmed the adequate separation of cytosolic and membrane fractions. In the same CG2 *pex5* mutant (ZP139), Pex5p was at a lower level regarding the total amount compared with that in CHO-K1 cells, mostly in the cytosolic fraction and less in the membrane fraction (Fig. 8*B*, *lanes 5* and *6*). In contrast, a larger amount of Pex5p was found in *pex2* Z65, *pex13* ZP128, and *pex12* ZP109, almost equally in both cytosolic and particulate fractions (*lanes 7–10*, *15*, and *16*). The localization of Pex5p in membrane fractions, including that in Z65, ZP109, and ZP128, was in good agreement with the findings by morphological analysis described above (Fig. 8*A*). In Pex14p-deficient ZP161 and *PEX7*-impaired ZPG207 (30), Pex5p was mostly in the cytosol, as in CHO-K1 cells (Fig. 8*B*, *lanes 11–14*).

To confirm the findings described above with respect to the intracellular location of Pex5p, PNS fractions from CHO-K1, Z65, ZP128, and ZP161 cells were fractionated by isopycnic sucrose density gradient ultracentrifugation. In CHO-K1 cells, Pex5p was nearly at the top of the gradient, and a small amount of Pex5p cosedimented with Pex14p, indicative of localization in peroxisomes (Fig. 8*C*). In Pex2p-defective Z65 (38), Pex5p was discernible nearly from the top to the middle of the gradient, where Pex14p representing peroxisomal remnants (20) sedimented to the middle. This was consistent with the recovery of more than half of Pex5p in the membrane fraction of Z65 (Fig. 8*B*, *lanes 7* and *8*). Similar sedimentation of Pex5p in the gradient was seen in the case of Pex13p-defective ZP128. Contrary to these two mutants, in Pex14p-deficient ZP161, most of Pex5p remained nearly at the top, whereas PMP70, a marker membrane protein for peroxisomal ghosts, was in the middle of the gradient. Collectively, Pex5p is localized in the peroxisomal remnants in *pex2* and *pex13* mutants (Z65 and ZP128, respectively), whereas Pex5p is mostly in soluble fractions in *pex14* ZP161, as in CHO-K1 cells. Thus, it is conceivable that Pex14p is required for targeting of Pex5p to peroxisomes.

Moreover, Pex5p found in the organellar fraction of Z65 was

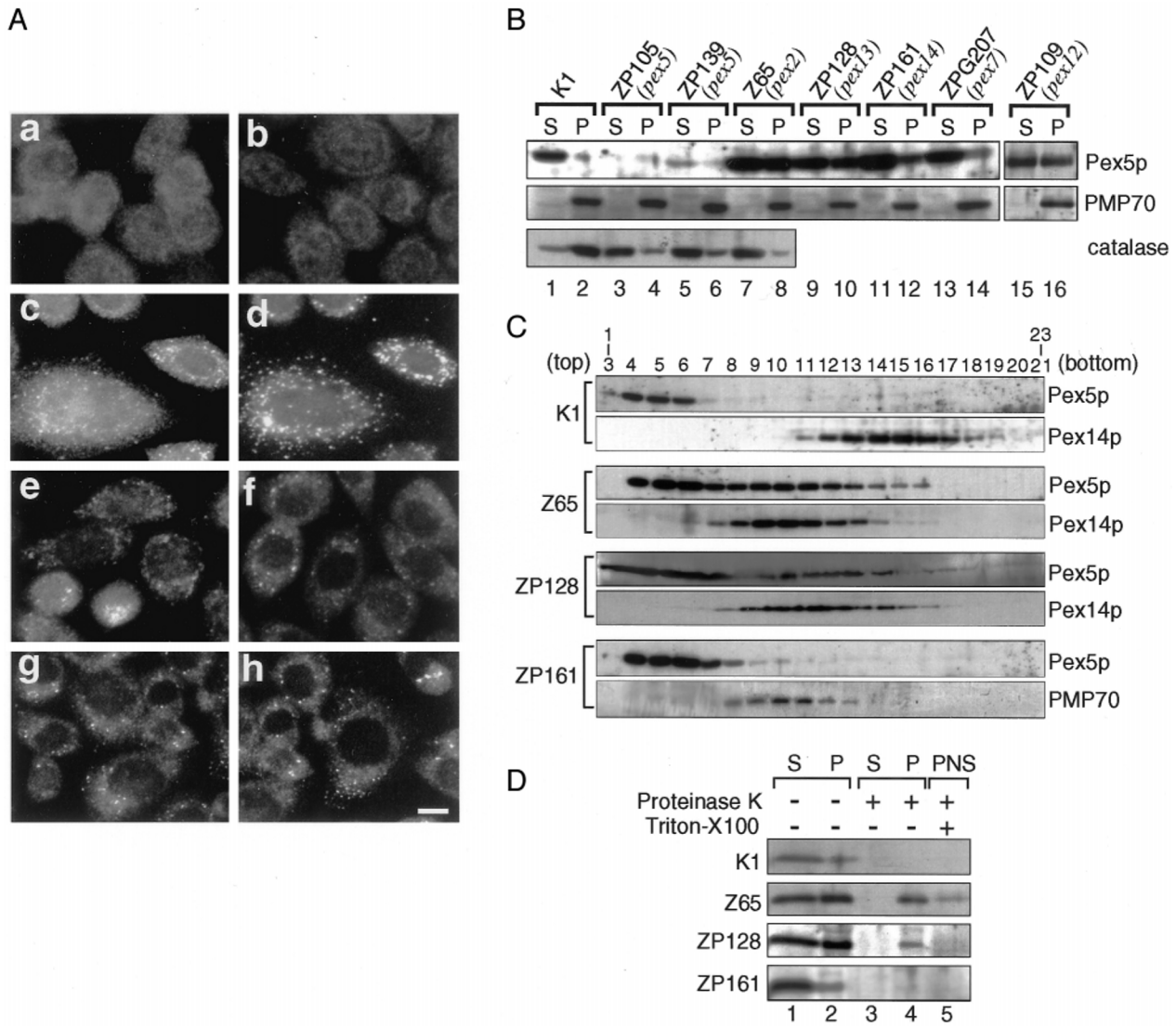

FIG. 8. **Intracellular localization of Pex5p.** *A*, morphological analysis. The intracellular location of Pex5p was analyzed by immunofluorescent staining of wild-type and mutant CHO cells. *PEX2*-defective Z65 cells that had been transfected with cDNA encoding N-terminally FLAG-tagged rat Pex12p (53) were also stained. The cells used were as follows: CHO-K1 (*panel a*), *pex14* ZP161 (*panel b*), Z65 (*panels c* and *d*), *pex12* ZP109 (*panels e* and *f*), and *pex13* ZP128 (*panels g* and *h*). Cells were treated with 1% Triton X-100 (*panels a*, *b*, *e*, and *g*) or 25 μg/ml digitonin (*panels c*, *d*, *f*, and *h*) and then stained with antibodies to Pex5p (*panels a–c* and *e–h*) and FLAG (*panel d*). Magnification × 630; *bar* = 20 μm. *B*, immunoblot analysis. Subcellular fractions of PNS fractions from CHO-K1, *pex5* ZP105 and ZP139, *pex2* Z65, *pex13* ZP128, *pex14* ZP161, *pex7* ZPG207, and *pex12* ZP109 cells (5×10^5 each) were subjected to SDS-PAGE. Cell types are indicated at the top: *S*, cytosolic fraction derived from the PNS; *P*, organellar fraction derived from the PNS. Immunoblot analysis was done with antibodies to Pex5p and PMP70. The *S* and *P* fractions from CHO-K1, ZP105, ZP139, and Z65 cells were also immunoblotted using anti-catalase antibody to assess the adequate separation of *S* and *P*. *C*, isopycnic subcellular fractionation. PNS fractions from CHO-K1, Z65, ZP128, and ZP161 cells were separately fractionated by isopycnic sucrose density gradient ultracentrifugation. The gradient was collected into 23 tubes. An equal volume (15 μl) of each fraction and of pooled fractions 1–3 and 21–23 was analyzed by SDS-PAGE, followed by immunoblotting with antisera to Pex5p, Pex14p, and PMP70 (only for Pex14p-deficient ZP161). Results are presented in the direction of lower to higher density of sucrose, from left to right. *D*, sensitivity to protease treatment. PNS fractions from CHO-K1, Z65, ZP128, and ZP161 cells were separately treated with proteinase K for 30 min on ice. The reaction was terminated with 1 mM phenylmethylsulfonyl fluoride. The reaction mixture was centrifuged to separate supernatant (*S*) and organellar (*P*) fractions. *S* and *P* fractions were analyzed as described for *B* using anti-Pex5p antibody. The PNS was mock-treated (*lanes 1* and *2*) or treated with 10 μg/ml proteinase K in the absence (*lanes 3* and *4*) or presence (*lane 5*) of 0.5% Triton X-100.

moderately resistant to treatment with exogenously added proteinase K, and part of membrane-associated Pex5p in Pex13p-deficient ZP128 was also resistant, under which conditions cytosolic Pex5p in both mutants was completely digested (Fig. 8*D*). However, Pex5p (in a rather smaller amount) in the membrane fractions of CHO-K1 and ZP161 cells was fully sensitive to proteinase K treatment. These results were interpreted to mean that the protease-resistant form of Pex5p is in the membrane of and/or inside the peroxisomal remnants in Z65 and ZP128, presumably representing the Pex5p stuck in the putative import machinery. The higher protease resistance, apparently indicative of being more deeply buried, of Pex5p in Pex2p-defective cells also implies that Pex2p functions as a component of the import machinery, downstream of Pex13p. It is possible that Pex5p partly localizes on the surface of peroxisomes in CHO-K1 cells and on the peroxisomal ghosts in ZP161 lacking Pex14p. Conceivably, Pex5p that was found accessible to the anti-Pex5p antibody after permeabilization of cell membranes with digitonin (Fig. 8*A*) may represent protease-sensitive Pex5p.

Accumulation of Pex5p in Pex14p Affects PTS1 and PTS2 Import

To search for a potential docking site of the apparently mobile receptor Pex5p, we took an approach to address whether

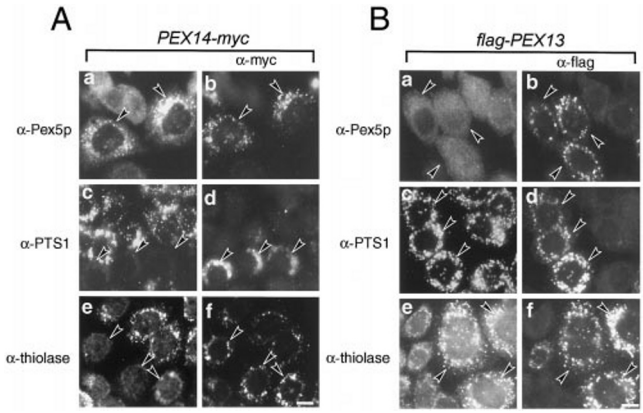

FIG. 9. **Overexpression of Pex14p affects the intracellular localization of Pex5p.** *A*, CHO-K1 cells were transfected with rat *PEX14-myc* and cultured for 2 days. Cells were treated with 25 μg/ml digitonin (*panels a* and *b*) or 1% Triton X-100 (*panels c–f*) and then stained with antibodies to Pex5p (*panel a*), Myc (*panels b*, *d*, and *f*), PTS1 (*panel c*), and thiolase (*panel e*). *Arrowheads* indicate the cells expressing Pex14p-Myc. Magnification × 630; *bar* = 20 μm. *B*, CHO-K1 cells were likewise transfected with Chinese hamster *FLAG-PEX13*. Cells were treated with 25 μg/ml digitonin (*panels a* and *b*) or 1% Triton X-100 (*panels c–f*) and stained with antibodies to Pex5p (*panel a*), FLAG (*panels b*, *d*, and *f*), PTS1 (*panel c*), and thiolase (*panel e*). *Arrowheads* indicate FLAG-Pex13p-expressing cells.

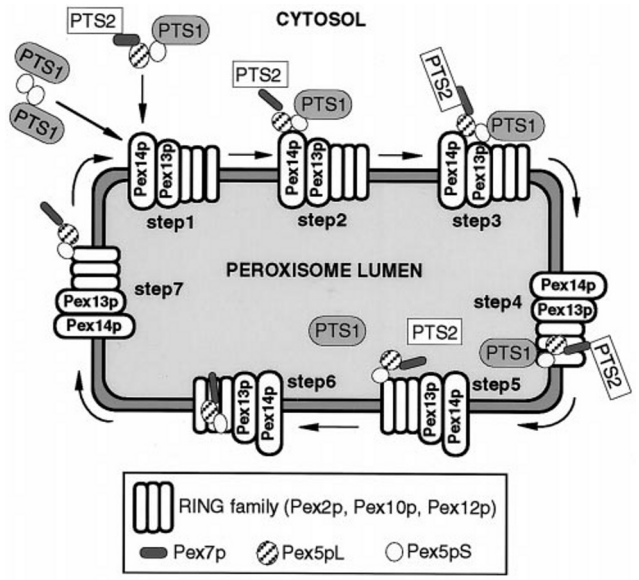

FIG. 10. **Schematic view of peroxisomal protein import mediated by shuttle translocator Pex5p.** In the cytosol are shown only the Pex5pS dimer·PTS1 proteins and Pex5pS/L·Pex7p·cargo proteins, each with PTS1 or PTS2, that represent several different forms of Pex5p, the PTS2 receptor Pex7p, and their cargo complexes to be formed. Pex5pL, in both homomeric and heteromeric dimers, equally binds PTS1 proteins and translocates to Pex14p. Pex5pL·Pex7p·PTS2, the Pex5pL dimer interacting with Pex7p and PTS2 proteins, likewise traverses and docks onto Pex14p. The signal receptors and cargo complexes translocate to the inner side of the potential import machinery, comprising Pex14p, Pex13p, and possibly RING peroxins: Pex2p, Pex10p, and Pex12p. PTS1 and PTS2 proteins are released at the inner surface and/or inside of peroxisomes. Both Pex5p and Pex7p then shuttle back to the cytosol.

overexpression of putative anchoring factors such as Pex14p causes a distinct change in the morphological phenotype of Pex5p. *PEX14-myc* encoding C-terminally Myc-tagged rat Pex14p and active in restoring peroxisomes in *PEX14*-impaired CHO mutants (20) was expressed under a strong promoter, SRα, in CHO-K1 cells. In Pex14p-Myc-expressing cells, the level of Pex14p-Myc was ~10-fold higher than that of endogenous Pex14p as assessed by immunoblotting (data not shown). Pex5p apparently accumulated in peroxisomal membranes, as seen in *pex2* Z65, *pex12* ZP109, and *pex13* ZP128 (see above), with which Pex14p-Myc was co-localized as assessed by immunostaining after digitonin treatment of cells (Fig. 9*A*, *panels a* and *b*). Strikingly, in Pex14p-Myc-positive cells, both PTS1 proteins and PTS2 thiolase were not in punctate structures, but mostly rather diffused in the cytosol (*panels c–f*), therefore demonstrating that import of PTS1 and PTS2, but not peroxisomal membrane proteins, was affected by overexpression of Pex14p and concomitant accumulation of Pex5p. A larger excess of Pex14p may also lead to an unbalanced assembly of a putative import machinery. In contrast, we found in CHO-K1 cells that nearly a 10-fold overexpression of FLAG-tagged Chinese hamster Pex13p relative to endogenous Pex13p caused no apparent accumulation of Pex5p, resulting in normal import of PTS1 proteins and PTS2 (Fig. 9*B*). Likewise, the intracellular location of Pex5p and import of PTS1 and PTS2 proteins were not affected in CHO-K1 cells overexpressing FLAG-tagged Pex10p or Pex12p (data not shown). Taken together, it is very likely that Pex5p binds to Pex14p at the first step in the import process of matrix polypeptides, including PTS1 and PTS2 proteins, into peroxisomes.

DISCUSSION

In addition to a defect in PTS1 transport, the typical phenotype of mammalian and yeast *pex5* mutants, the impaired PTS2 import in *pex5* mutants of mammals (including fibroblasts from a CG2 Zellweger syndrome patient), and its restoration by Pex5pL are the novel findings (11, 12). As a step toward addressing this issue, we recently demonstrated that Pex14p binds both isoforms of Pex5p (Pex5pS and Pex5pL) and, with their cargo, PTS1 protein as well as Pex7p with PTS2 protein (20). In the present work, we showed that both Pex5pS and Pex5pL, in a homomeric and/or heteromeric dimer, bind to PTS1 proteins. More strikingly, studies *in vivo* as well as *in vitro* demonstrated that Pex5pL interacts with PTS2 protein in a Pex7p-mediated manner, with a concomitant increase in PTS2 protein bound per Pex7p, implying the dual function of Pex5p in mammals, *i.e.* transport of both PTS1 and PTS2 proteins. Pex5pL directly binds to Pex7p, whereby a Pex5pL homodimer or a heterodimeric form with Pex5pS transports the PTS2 proteins. In contrast, in yeast, an indirect interaction of Pex5p with Pex7p, apparently requiring Pex14p, was found (46).

The intracellular location of Pex7p is still under debate, particularly in *Saccharomyces cerevisiae*, arguing that Pex7p is mostly in the cytosol (47) or is intraperoxisomal (48). In human cells, overexpression of human Pex7p resulted in its localization exclusively in the cytosol (49). In the present work, we also observed such an intracellular location of Pex7p in 207P7 cells, stable human *PEX7* transfectants of a PTS2-GFP-transformed CHO *pex7* mutant, ZPG207 (Fig. 7*A*). To elucidate the physiological consequence of the interaction between Pex5pL and Pex7p, we investigated whether Pex5pL affects the intracellular localization of Pex7p. The higher level of Pex5pL expression gave rise to peroxisomal accumulation of Pex7p and enhanced PTS2-GFP import in 207P7 cells, evidently demonstrating that Pex5pL functions in the transport of the Pex7p·PTS2 complex. It is noteworthy that structurally and functionally homologous peroxins, *S. cerevisiae* Pex18p and Pex21p, were recently isolated as factors required for targeting of Pex7p and PTS2 to peroxisomes (50). It is tempting to speculate that Pex5pL functions like these peroxins in the transport of Pex7p and PTS2. It is also possible that the orthologues of yeast Pex18p and Pex21p may exist in mammals.

The ZP105-type mutation G335E in TPR1 reduces the activity of Pex5pL in recognizing PTS1, whereas ZP139-derived

Pex5pL with the mutation G522E in TPR6 is incapable of binding PTS1. However, both Pex5pL mutants are indistinguishable from wild-type Pex5pL in binding to Pex7p. These findings can explain the ZP139-type phenotype showing the defect in import of PTS1, but not PTS2 (11). A similar phenotype was noted in fibroblasts from a CG2 patient with neonatal adrenoleukodystrophy with the missense mutation N489K in Pex5pS (N526K in Pex5pL) (9, 12). The undetectable level of Pex5p in ZP105 owing to its degradation apparently reflects the phenotype, an impaired import of both PTS1 and PTS2. It is noteworthy that *PEX5* mRNA with an intragenic termination codon (R390Ter) was under the detectable level in a CG2 Zellweger syndrome patient manifesting PTS1 and PTS2 import defects (12). Pex5pL-G335E is active *in vivo* as well in interacting with the Pex7p·PTS2 complex, as witnessed in complementation of PTS2 import in ZP105 in a *ts* manner and by its overexpression. Given the fact that import of both PTS1 and PTS2 is affected in ZP105 cells presumably possessing functional Pex7p and Pex14p, one of the two potential translocation pathways, namely Pex14p-Pex5pL-Pex7p-PTS2 protein, is likely to be mainly utilized for PTS2 import *in vivo*, rather than the import route of Pex14p-Pex7p-PTS2 protein. It is of interest to note that Pex5p is also extensively reduced in *PEX1*- and *PEX6*-deficient patient fibroblasts (51) and CHO cell mutants,[5] although the relationship of Pex1p and Pex6p of the ATPases associated with diverse cellular activities (AAA) protein family to Pex5p has not been elucidated.

With respect to the oligomerization of Pex5p, our observation that Pex5pS and Pex5pL form a homomeric as well as a heteromeric dimer is not compatible with the recent finding describing a homotetramer of recombinant His_6-tagged human Pex5pL and Pex5pS (52). In the size estimation by the gel filtration method, 1) we used Chinese hamster Pex5pS purified from bacterially expressed GST fusion protein; 2) we incubated Pex5p at pH 7.4 rather than pH 8.0 (52); and 3) in addition to recombinant protein, we also used the cytosol from rat liver. The data obtained led us to conclude that Pex5p forms a dimer. In the present study, homomeric and heteromeric type association of Pex5p was verified *in vitro* using cell-free synthesized Chinese hamster ^{35}S-labeled Pex5p and HA-tagged Pex5p expressed in wild-type CHO cells or the *pex5* mutant. Furthermore, in *pex5* mutant ZP139 deficient in PTS1 import but PTS2 import-competent (11), even expression of Pex5pS enhanced peroxisomal localization of PTS2 protein (thiolase), presumably by fully using endogenous Pex5pL-G522E (data not shown). Therefore, it is conceivable that Pex5p forms not only a homomeric dimer, but also a heteromeric form, whereby only the dimers including Pex5pL play a role in PTS2 transport. It is less likely, however, that Pex5p forms different types of oligomers between the mammalian species, Chinese hamster and rat *versus* humans. The discrepancy between homo/heterodimers of Pex5p and a homotetramer, independently concluded by two groups of investigators (this work; 52), remains to be addressed. In either event, the oligomerization of Pex5p may also accommodate an import receptor adaptive from a normal level to highly induced state, such as that by potent peroxisome proliferators (Fig. 1*A*) of peroxisomal proteins. The dimeric form of recombinant Pex5pS indeed shows a higher affinity for acyl-CoA oxidase as acyl-CoA oxidase concentration increases.[6]

Pex5p is located mostly in the cytosol in normal CHO cells and *PEX7*-impaired ZPG207 (30), both expressing functional Pex5p and Pex14p. In contrast, Pex5p accumulates in peroxisomal remnants in CHO mutants, *pex2* Z65 (38), *pex12* ZP109 (31, 53), and *pex13* ZP128 (23), possibly caused by interference in shuttling between the cytosol and peroxisomes. Such abnormal localization of Pex5pS and Pex5pL apparently reflects the phenotype of import defects of PTS1 and PTS2, owing to a blockade of the import pathway(s), plausibly in addition to the dysfunction of each peroxin in the respective cell mutant. It is possible that these peroxins may play an important role in the export of Pex5p from peroxisomes to the cytoplasm. Similar accumulation of Pex5p in peroxisomal ghosts was noted in fibroblasts from PBD patients of several complementation groups such as *PEX12*-defective CG3 and *PEX2*-impaired CG10 (51). Moreover, Pex5p is localized as a protease-resistant form in Z65 and ZP128 and as an antibody-inaccessible one after digitonin treatment in *PEX10*-defective CG7 patient fibroblasts (51, 54), suggesting that Pex5p is stuck inside the remnants and/or in the membrane, plausibly causing an impaired recycle-back to the cytosol. Conversely, Pex5p is stable in the cytosol in Pex14p-deficient ZP161 (20) as in CHO-K1 cells, whereas ZP161 shows a typical mutant phenotype, *i.e.* the impaired import of PTS1 and PTS2, possibly owing to the loss of the Pex5p-anchoring factor. The reverse, overexpression of Pex14p, results in a striking increase in Pex5p accumulated in peroxisomes and the concomitantly affected import of PTS1 and PTS2. No such phenotype was envisaged in CHO cells overexpressing Pex13p, Pex12p, or Pex10p. Therefore, Pex14p appears to function at the earliest and prerequisite step as a docking site of Pex5p carrying its cargoes, PTS1 and PTS2 matrix proteins, but not membrane polypeptides, thereby playing a pivotal role in the peroxisome assembly processes. A similar schematic view of Pex14p has recently been suggested (20, 21, 55). Furthermore, given the fact that Pex5p not only accumulates in peroxisomal remnants in *PEX2*-, *PEX10*-, and *PEX12*-defective mutant cells, but also interacts with Pex12p, it is conceivable that the RING peroxins Pex2p, Pex10p, and Pex12p function as a part of the putative translocation machinery, downstream of Pex14p and Pex13p. Similar findings using *PEX12*-impaired PBD patient fibroblasts have been recently reported (56).

Based on the data we reported here, we propose a schematic model of a peroxisomal import machinery tightly linked to the function of Pex5p (Fig. 10). The receptor and cargo complexes, including Pex5p dimer·PTS1 proteins, Pex5p·Pex7p·PTS2 proteins, and Pex5p·Pex7p·cargo proteins, each with PTS1 or PTS2, are formed in the cytosol, traverse to peroxisomes, bind to Pex14p in the potential translocation machinery, and translocate to Pex13p subsequently to the RING peroxins. The interaction of Pex5pS and Pex5pL with Pex14p does not require Pex13p, although we do not know whether the interaction noted between Pex5p and Pex13p as well as Pex14p and Pex13p is direct or is mediated by other peroxisomal proteins. After emerging at the matrix side of the machinery, PTS1 and PTS2 proteins will be released from the receptors. PTS1 and PTS2 can be simultaneously and/or independently imported, as noted in *pex5* ZP139 showing a defect in only PTS1 import, but not PTS2 import (11), as well as in *pex7* ZPG207 solely deficient in PTS2 import (30). Import of PTS1 and PTS2 is likely to share the common, if not exclusive, translocon, as inferred from the common phenotype, the impaired import of both PTS1 and PTS2, in CHO cell mutants *pex2*, *pex12*, *pex13*, and *pex14*. It is also plausible that Pex7p translocates into peroxisomes, as shown in yeast (57). At the last step of protein import, Pex5p and Pex7p in a bound form or independently cycle back to the cytosol.

Acknowledgments—We thank S. Tamura for advice on the isopycnic centrifugation and other members of the Fujiki laboratory for discussion. We also thank N. Thomas for comments.

[5] S. Tamura and Y. Fujiki, unpublished data.

[6] T. Harano and Y. Fujiki, manuscript in preparation.

REFERENCES

1. van den Bosch, H., Schutgens, R. B. H., Wanders, R. J. A., and Tager, J. M. (1992) *Annu. Rev. Biochem.* **61,** 157–197
2. Fujiki, Y. (1997) *Biochim. Biophys. Acta* **1361,** 235–250
3. Lazarow, P. B., and Fujiki, Y. (1985) *Annu. Rev. Cell Biol.* **1,** 489–530
4. Titorenko, V. I., and Rachubinski, R. A. (1998) *Trends Biochem. Sci.* **23,** 231–233
5. Distel, B., Erdmann, R., Gould, S. J., Blobel, G., Crane, D. I., Cregg, J. M., Dodt, G., Fujiki, Y., Goodman, J. M., Just, W. W., Kiel, J. A. K. W., Kunau, W.-H., Lazarow, P. B., Mannaerts, G. P., Moser, H., Osumi, T., Rachubinski, R. A., Roscher, A., Subramani, S., Tabak, H. F., Tsukamoto, T., Valle, D., van der Klei, I., van Veldhoven, P. P., and Veenhuis, M. (1996) *J. Cell Biol.* **135,** 1–3
6. Erdmann, R., Veenhuis, M., and Kunau, W.-H. (1997) *Trends Cell Biol.* **7,** 400–407
7. Kunau, W.-H. (1998) *Curr. Opin. Microbiol.* **1,** 232–237
8. Subramani, S. (1997) *Nat. Genet.* **15,** 331–333
9. Dodt, G., Braverman, N., Wong, C. S., Moser, A., Moser, H. W., Watkins, P., Valle, D., and Gould, S. J. (1995) *Nat. Genet.* **9,** 115–125
10. Wiemer, E. A., Nuttley, W. M., Bertolaet, B. L., Li, X., Francke, U., Wheelock, M. J., Anne, U. K., Johnson, K. R., and Subramani, S. (1995) *J. Cell Biol.* **130,** 51–65
11. Otera, H., Tateishi, K., Okumoto, K., Ikoma, Y., Matsuda, E., Nishimura, M., Tsukamoto, T., Osumi, T., Ohashi, K., Higuchi, O., and Fujiki, Y. (1998) *Mol. Cell. Biol.* **18,** 388–399
12. Braverman, N., Dodt, G., Gould, S. J., and Valle, D. (1998) *Hum. Mol. Genet.* **7,** 1195–1205
13. McCollum, D., Monosov, E., and Subramani, S. (1993) *J. Cell Biol.* **121,** 761–774
14. Van der Leij, I., Franse, M. M., Elgersma, Y., Distel, B., and Tabak, H. F. (1993) *Proc. Natl. Acad. Sci. U. S. A.* **90,** 11782–11786
15. van der Klei, I. J., Hilbrands, R. E., Swaving, G. J., Waterham, H. R., Vrieling, E. G., Titorenko, V. I., Cregg, J. M., Harder, W., and Veenhuis, M. (1995) *J. Biol. Chem.* **270,** 17229–17236
16. Szilard, R. K., Titorenko, V. I., Veenhuis, M., and Rachubinski, R. A. (1995) *J. Cell Biol.* **131,** 1453–1469
17. Elgersma, Y., Kwast, L., Klein, A., Voorn-Brouwer, T., van den Berg, M., Metzig, B., America, T., Tabak, H. F., and Distel, B. (1996) *J. Cell Biol.* **135,** 97–109
18. Erdmann, R., and Blobel, G. (1996) *J. Cell Biol.* **135,** 111–121
19. Gould, S. J., Kalish, J. E., Morrell, J. C., Bjorkman, J., Urquhart, A. J., and Crane, D. I. (1996) *J. Cell Biol.* **135,** 85–95
20. Shimizu, N., Itoh, R., Hirono, Y., Otera, H., Ghaedi, K., Tateishi, K., Tamura, S., Okumoto, K., Harano, T., Mukai, S., and Fujiki, Y. (1999) *J. Biol. Chem.* **274,** 12593–12604
21. Albertini, M., Rehling, P., Erdmann, R., Girzalsky, W., Kiel, J. A. K. W., Veenhuis, M., and Kunau, W.-H. (1997) *Cell* **89,** 83–92
22. Brocard, C., Lametschwandtner, G., Koudelka, R., and Hartig, A. (1997) *EMBO J.* **16,** 5491–5500
23. Toyama, R., Mukai, S., Itagaki, A., Tamura, S., Shimozawa, N., Suzuki, Y., Kondo, N., Wanders, R. J. A., and Fujiki, Y. (1999) *Hum. Mol. Genet.* **8,** 1673–1681
24. Shimozawa, N., Suzuki, Y., Zhang, Z., Imamura, A., Toyama, R., Mukai, S., Fujiki, Y., Tsukamoto, T., Osumi, T., Orii, T., Wanders, R. J. A., and Kondo, N. (1999) *Hum. Mol. Genet.* **8,** 1077–1083
25. Liu, Y., Bjoerkman, J., Urquhart, A., Wanders, R. J. A., Crane, D. I., and Gould, S. J. (1999) *Am. J. Hum. Genet.* **65,** 621–634
26. Tateishi, K., Okumoto, K., Shimozawa, N., Tsukamoto, T., Osumi, T., Suzuki, Y., Kondo, N., Okano, I., and Fujiki, Y. (1997) *Eur. J. Cell Biol.* **73,** 352–359
27. Ghaedi, K., Itagaki, A., Toyama, R., Tamura, S., Matsumura, T., Kawai, A., Shimozawa, N., Suzuki, Y., Kondo, N., and Fujiki, Y. (1999) *Exp. Cell Res.* **248,** 482–488
28. Tsukamoto, T., Yokota, S., and Fujiki, Y. (1990) *J. Cell Biol.* **110,** 651–660
29. Imamura, A., Tamura, S., Shimozawa, N., Suzuki, Y., Zhang, Z., Tsukamoto, T., Orii, T., Kondo, N., Osumi, T., and Fujiki, Y. (1998) *Hum. Mol. Genet.* **7,** 2089–2094
30. Ghaedi, K., Kawai, A., Okumoto, K., Tamura, S., Shimozawa, N., Suzuki, Y., Kondo, N., and Fujiki, Y. (1999) *Exp. Cell Res.* **248,** 489–497
31. Okumoto, K., Shimozawa, N., Kawai, A., Tamura, S., Tsukamoto, T., Osumi, T., Moser, H., Wanders, R. J. A., Suzuki, Y., Kondo, N., and Fujiki, Y. (1998) *Mol. Cell. Biol.* **18,** 4324–4336
32. Kinoshita, N., Ghaedi, K., Shimozawa, N., Wanders, R. J. A., Matsuzono, Y., Imanaka, T., Okumoto, K., Suzuki, Y., Kondo, N., and Fujiki, Y. (1998) *J. Biol. Chem.* **273,** 24122–24130
33. Honsho, M., Tamura, S., Shimozawa, N., Suzuki, Y., Kondo, N., and Fujiki, Y. (1998) *Am. J. Hum. Genet.* **63,** 1622–1630
34. Miura, S., Miyazawa, S., Osumi, T., Hashimoto, T., and Fujiki, Y. (1994) *J. Biochem.* (*Tokyo*) **115,** 1064–1068
35. Miyazawa, S., Osumi, T., Hashimoto, T., Ohno, K., Miura, S., and Fujiki, Y. (1989) *Mol. Cell. Biol.* **9,** 83–91
36. Hess, R., Staubli, W., and Reiss, W. (1965) *Nature* **208,** 856–858
37. Rachubinski, R. A., Fujiki, Y., Mortensen, R. M., and Lazarow, P. B. (1984) *J. Cell Biol.* **99,** 2241–2246
38. Tsukamoto, T., Shimozawa, N., and Fujiki, Y. (1994) *Mol. Cell. Biol.* **14,** 5458–5465
39. Imamura, A., Tsukamoto, T., Shimozawa, N., Suzuki, Y., Zhang, Z., Imanaka, T., Fujiki, Y., Orii, T., Kondo, N., and Osumi, T. (1998) *Am. J. Hum. Genet.* **62,** 1539–1543
40. Shimozawa, N., Tsukamoto, T., Suzuki, Y., Orii, T., and Fujiki, Y. (1992) *J. Clin. Invest.* **90,** 1864–1870
41. Tamura, S., Okumoto, K., Toyama, R., Shimozawa, N., Tsukamoto, T., Suzuki, Y., Osumi, T., Kondo, N., and Fujiki, Y. (1998) *Proc. Natl. Acad. Sci. U. S. A.* **95,** 4350–4355
42. Miyazawa, S., Hayashi, H., Hijikata, M., Ishii, N., Furuta, S., Kagamiyama, H., Osumi, T., and Hashimoto, T. (1987) *J. Biol. Chem.* **262,** 8131–8137
43. Furuta, S., Hayashi, H., Hijikata, M., Miyazawa, S., Osumi, T., and Hashimoto, T. (1986) *Proc. Natl. Acad. Sci. U. S. A.* **83,** 313–317
44. Purdue, P. E., and Lazarow, P. B. (1996) *J. Cell Biol.* **134,** 849–862
45. Tsukamoto, T., Miura, S., and Fujiki, Y. (1991) *Nature* **350,** 77–81
46. Girzalsky, W., Rehling, P., Stein, K., Kipper, J., Blank, L., Kunau, W.-H., and Erdmann, R. (1999) *J. Cell Biol.* **144,** 1151–1162
47. Rehling, P., Marzioch, M., Niesen, F., Wittke, E., Veenhuis, M., and Kunau, W.-H. (1996) *EMBO J.* **15,** 2901–2913
48. Zhang, J. W., and Lazarow, P. B. (1996) *J. Cell Biol.* **132,** 325–334
49. Braverman, N., Steel, G., Obie, C., Moser, A., Moser, H., Gould, S. J., and Valle, D. (1997) *Nat. Genet.* **15,** 369–376
50. Purdue, P. E., Yang, X., and Lazarow, P. B. (1998) *J. Cell Biol.* **143,** 1859–1869
51. Dodt, G., and Gould, S. J. (1996) *J. Cell Biol.* **135,** 1763–1774
52. Schliebs, W., Saidowsky, J., Angianian, B., Dodt, G., Herberg, F. W., and Kunau, W.-H. (1999) *J. Biol. Chem.* **274,** 5666–5673
53. Okumoto, K., and Fujiki, Y. (1997) *Nat. Genet.* **17,** 265–266
54. Okumoto, K., Itoh, R., Shimozawa, N., Suzuki, Y., Tamura, S., Kondo, N., and Fujiki, Y. (1998) *Hum. Mol. Genet.* **7,** 1399–1405
55. Will, G. K., Soukupova, M., Hong, X., Erdmann, K. S., Kiel, J. A. K. W., Dodt, G., Kunau, W.-H., and Erdmann, R. (1999) *Mol. Cell. Biol.* **19,** 2265–2277
56. Chang, C.-C., Warren, D. S., Sacksteder, K. A., and Gould, S. J. (1999) *J. Cell Biol.* **147,** 761–773
57. Elgersma, Y., Elgersma-Hooisma, M., Wenzel, T., McCaffery, J. M., Farquhar, M. G., and Subrmani, S. (1998) *J. Cell Biol.* **140,** 807–820